Review:

Semiconductor Gas Sensors: Metal Oxides, Synthesis Methods, Applications as Gas Sensors, and Oxidation and Reduction Mechanisms

Inam Abed Hammod[1,2*], Noor Jawad Ridha[1], Khawla Jemeel Tahir[1], Firas Kamel Mohamad Alosfur[1], Asaad Sabbar Yasir[1], and Luma Ahmed Majeed[1]

[1]*Department of Physics, College of Science, University of Kerbala, Karbala 56001, Iraq*

[2]*Department of Physiology and Medical Physics, College of Medicine, University of Kerbala, Karbala 56001, Iraq*

* ***Corresponding author:***

tel: +964-7808120446
email: inam.a@uokerbala.edu.iq

Received: March 22, 2024
Accepted: August 19, 2024

DOI: 10.22146/ijc.95018

Abstract: *Over the last several decades, advancements in industry have facilitated the absorption of harmful gases into the bloodstream or lungs via dermal absorption or inhalation. This process may elicit diverse cellular responses, potentially leading to adverse health effects. Consequently, air pollution has emerged as a significant worldwide issue. Hence, developing a device capable of monitoring air pollution and detecting these chemicals in the surrounding environment became imperative. Gas sensors are instruments used for regulating industrial emissions, surveillance of environmental contaminants, and identification of pollutants and hazardous gases. Semiconductor gas sensors have garnered significant recognition owing to their several advantageous characteristics, including simplified production processes, compact dimensions, and low-cost. Some of its drawbacks include limited selectivity and high operating temperatures. This review discusses the most often used semiconducting materials in gas sensing, as well as the methods used to synthesize them, and the reduction and oxidation processes that happen between metal oxides and analyte gas. Furthermore, the various strategies employed to increase the gas-sensing response are explored, such as doping with noble metals and the formation of heterostructures.*

Keywords: *gas sensor; semiconductor; metal oxides; synthesis methods; heterojunction*

■ INTRODUCTION

Due to the dangerous effects of gases on the environment and health, the detection of toxic gases has gained popularity because of fast technological and industrial advancement, which leads to outdoor and indoor environmental pollution and several harmful health effects. According to the World Health Organization, air pollution in 2012 was largely due to toxic gases, which resulted in ~7.106 early deaths [1-3]. Furthermore, indoor environments contain a multitude of volatile organic compounds (VOCs), including but not limited to methanol (CH_3OH), benzene (C_6H_6), acetone (CH_3COCH_3), ethanol (C_2H_5OH), and toluene ($C_6H_5CH_3$), alongside inorganic gases such as carbon dioxide (CO_2), nitrous oxides (NO_x), and carbon monoxide (CO). In recent years, advancements in industrial sectors have increased recognition of the potential for hazardous gases to enter the human body by skin absorption or inhalation; subsequently entering the bloodstream or lungs may cause various cellular reactions and potentially give rise to health complications. It was necessary to design a gadget to effectively monitor air pollution and detect various substances in the surrounding environment [4]. Numerous conventional approaches include the development of detecting devices that utilize auditory signals to alert individuals to the presence of hazardous gases. However, the reliability of these approaches is questionable due to the necessity of obtaining precise, real-time measurements of the concentration of the gas being targeted. Gas sensors play a significant role in this

field and attract more attention because they turn the gas volume portion into an electrical signal. Numerous types of sensors have been studied and developed depending on different sensor materials and manufacturing methods [5].

According to the material of the sensor and its basic principle, gas sensors are categorized as semiconductors. This sensor is distinguished by its ability to detect various gases (transient organic compounds or inorganic compounds) at low concentrations in the range of part per million (ppm) or part per billion (ppb). Metal oxide semiconductors (MOSs) are based on two functions that define their fundamental principle: first, the chemical reaction that occurs between sensing materials and target gases, and second, the conversion of this chemical reaction into electrical signals due to a change in resistance [6]. Catalytic sensors are the second type of gas sensor utilized to detect combustible gases. This gaseous mixture remains non-combustible until it reaches a specific temperature threshold; however, the gas will ignite at lower temperature values in a chemical reaction [7]. Electrochemical sensors exhibit high durability and can detect low quantities of harmful gases that adversely affect human health. This particular sensor is designed to quantify alterations in electrical current that may arise upon exposure to various gases [8]. Another type was infrared sensors. The infrared sensor is vital in detecting environmental gases such as CH_4, CO_2, and CO. The gas system relies on an infrared light source that emits wavelengths within the 0.3 to 25.0 μm range. The technique can be classified into indirect and direct detections based on variations in the conversion of light energy. These devices employ an infrared light transmitter connected to a detector that operates at the specific wavelength of the gas being analyzed, enabling control over its wavelength [9]. The acoustic wave gas sensor, also known as a surface acoustic wave sensor, is a distinct type of sensor that relies on the orientation of wave propagation. The principle underlying the operation of these sensors is based on converting the input signal into mechanical waves, which are subsequently transformed back into electrical signals through the utilization of interdigitated transducers manufactured on a piezoelectric substrate [10]. In addition, many different types of sensors, such as chemical sensors, play a main role in our lives. Colorimetric sensors based on plasmonic nanostructures have attracted significant attention among chemical sensors using nanostructured materials. Localized surface plasmon resonance (SPR)-based sensors enable quick and accurate measurement of many analytes [11]. The SPR sensors work by sensing the frequency of oscillating electrons in the surroundings of plasmonic nanoparticles [12]. Nanosensor based on the SPR of metallic nanoparticles have gained popularity for detecting various chemical and biological species. The excitation of surface plasmons is strongly dependent on the refractive index of the dielectric medium; consequently, any interaction between the analyte and the plasmonic nanoparticle might alter the resonance state. This approach has been widely used to build accurate sensors for detecting metal ions in aqueous solutions. Recently, various studies have been done on the immobilized plasmonic nanosensor to identify heavy metals [13-14].

Due to their size-dependent chemical and physical characteristics, metal oxides are promising materials for several technological applications. These features include ease of manufacture, small size, low cost, and a high limit of detection [15]. Nanomaterials can increase the performance of MOS sensors by providing a large surface area, which produces more active reaction sites, or by combining various semiconducting metal oxides. The design of the metal oxide gas sensor is based on adsorption between semiconductor materials and gas molecules, which causes a change in electrical conductivity when a gas flows through it at temperatures ranging from 100 to 300 °C. Some disadvantages of MOS sensor technology include high operating temperatures, a lack of stability, and poor selectivity. As a result, several methods have been created to address these shortcomings [16]. The high consumption temperature, which varies between 200–500 °C, requires the presence of a heater in the sensor design to provide the thermal energy necessary for establishing the interaction between oxygen molecules and sensor material. Researchers have made many attempts to design a sensor that can operate at low temperatures. The

electronic characterization of MOS may be altered by exposing them to UV light, which modulates the carrier concentration [17]. Yuan et al. [18] demonstrated that the shape and structure of the material have an influence on the characteristics of the sensor. It turned out that the one-dimensional nanomaterial is more suitable for gas sensors. Also, Alamri et al. [19] used carbon nanotubes (MWCNT) as multiwall doping with Pt nanoparticles as H_2 gas sensors and illustrated the role of contact between materials in improving sensitivity and long-term stability. To achieve sensors with high selectivity, some researchers used noble metals as doping with metal oxides; others used loading. Although there are many reviews in the field of semiconductor gas sensors, in this review, we have focused on a brief survey of the important metal oxides used as gas sensing materials and their synthesis methods with mechanisms of oxidation and reduction.

■ MOS GAS SENSORS

In the literature, several metal oxides have been described and employed. After the second part of the 20th century, in 1952, germanium was the first semiconductor material used as a sensor material by Guan et al. [20]. Many semiconducting oxides (n-type) such as like SnO_2 [21-22], zinc oxide (ZnO) [23-24], indium oxide (In_2O_3) [25], and p-type like copper oxide (CuO) [26] reduced graphene oxide (rGO) [27] tungsten trioxide (WO_3) [28-29] have been used in the gas sensor as a sensing film. The evaluation of gas sensors may be performed by considering many indications, including operational temperature, stability, sensitivity, selectivity, recovery time, and response time [30]. Sensitivity is the ratio of the conductivity of the sensor in the presence of analysis gas to its conductivity in air. The sensitivity of the MOS sensor can be influenced by changing the structure, such as the porosity and grain size of the MOS sensor or by introducing impurities and dopants, like noble metals, metal oxides, or functionalization of the surface with noble metals. Modifying the oxide structure through the formation of heterostructures is considered one of the strategies for enhancing the sensor's sensitivity and selectivity [31]. Fig. 1 illustrates the schematic diagram of a gas sensor system.

■ SEMICONDUCTORS AS SENSING MATERIALS

Numerous materials have been investigated and utilized for the implementation of gas sensors. The properties of metal oxides as sensor materials can be improved by doping [32], for example, Zn/doped Fe_2O_3 [33], Sm/doped $CoFe_2O_4$ [34], and Nb/doped TiO_2 [35-36]. The conductivity of a semiconductor can be altered based on the kind of the semiconductor [20]. In this review, we present studies on various MOS from the literature.

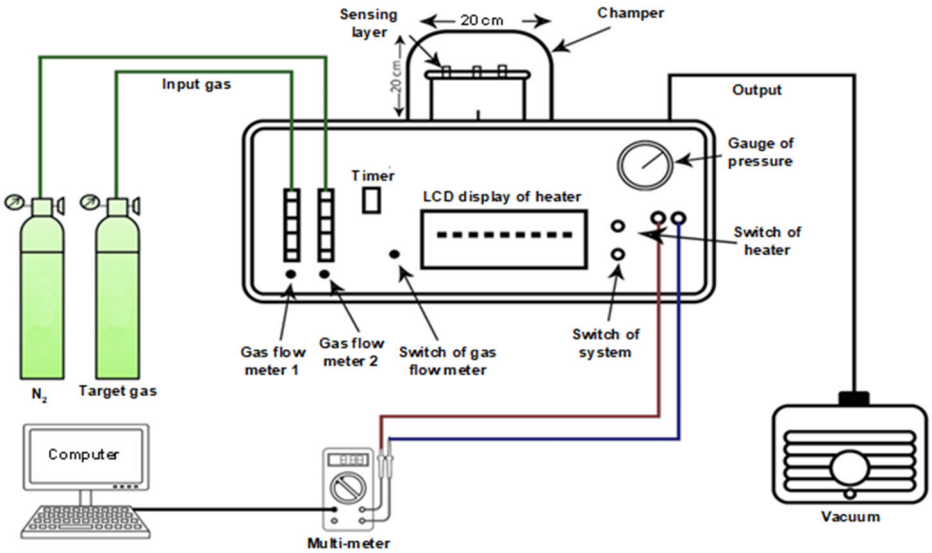

Fig 1. Schematic diagram for gas sensor system

SnO_2

The use of SnO_2 nanostructures as sensing materials in gas sensors has garnered significant attention attributed to its notable qualities, including high sensitivity, convenient production process, robust mechanical properties, and cost-effectiveness. It possesses interesting chemical and physical characteristics, including conductivity based on free electrons with a 3.6 eV band gap (Fig. 2) [37]. However, it suffers from low selectivity and high operating temperatures. To improve gas sensor-based SnO_2, researchers focus on surface modification, doping, morphology, or size control [38]. Many researchers have worked to reduce these drawbacks and have devoted their efforts to developing SnO_2 sensors with the lowest temperatures, either by doping with another metal mentioned above or by forming a composite with another metal oxide [39]. For example, Chen et al. [40] fabricated a high response-H_2S gas sensing by doping Cu with SnO_2-rGO via a simple solvothermal method. A subsequent annealing procedure was carried out after the synthesis process at 400 °C for 2 h. The sensor's sensitivity of around 156.7 at 120 °C was observed when detecting 10 ppm H_2S gas. The observed high sensitivity value can be attributed to a p-n-p heterostructure offering numerous adsorption sites and vacancies.

Additionally, incorporating Cu contributes to an increased surface area, while the proximity of a small grain size near Debye length enhances the sensor's performance. Furthermore, utilizing a large pore size facilitates faster response and recovery times for the sensor. Ayesh et al. [41] deposited a CuO-SnO_2 composite on a glass substrate. The sensor was tested on H_2S gas and showed excellent sensitivity to 10 ppm, due to the formation of CuS while the sensor film exposed to the H_2S. CuS can break the connection between CuO and SnO_2 and the band structure changes, then the electronic structure of SnO_2 returns to its original state. Guo et al. [42] used an electrospinning technique to produce SnO_2/ZnO. From this study, the response of this composite at room temperature to 0.5 ppm NO_2 gas was found to be around 336%, which was greater than the response of pure SnO_2 (13%), due to the heterojunction. Rodiawan et al. [43] mixed SnO_2 with gold via wet chemical method. The response of 1 ppm of H_2S gas was about 87.34 at 200 °C. The observed increase in response may be attributed to the formation of a Schottky barrier at the interface between Au and SnO_2, which arises from the distinction in the work functions of SnO_2 and Au.

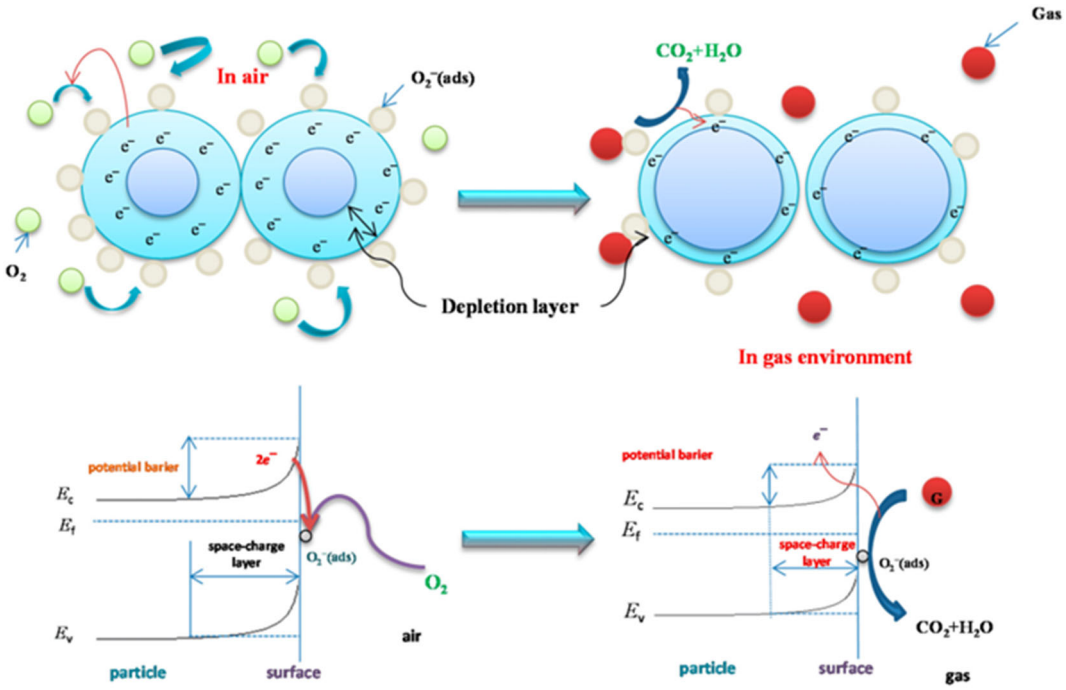

Fig 2. Sensing mechanism of SnO_2 for reducing gas [37].

CuO

CuO is a semiconductor with p-type conductivity, characterized by a bandgap ranging from 1.2 to 1.5 eV. CuO has distinctive properties such as superconductivity, thermal stability, robust electrochemical behavior, low manufacturing cost, and photovoltaic properties. In addition, CuO is present in a variety of phases: CuO, Cu_2O and Cu_4O_3. However, CuO and Cu_2O phases are more effective in the gas sensor area [44]. Researchers have recently reported that CuO are a thin film used in gas sensors to detect many gases. Peng et al. [45] used a simple hydrothermal technique to fabricate a CuO sensor. The sensor response primarily depended on the concentration of H_2S gas and the sensor's working temperature. The 5 ppm H_2S gas response was 10.9 at 150 °C, more than the other gases, demonstrating the H_2S gas's remarkable selectivity. Impurities and heterojunctions with other oxides can be introduced to improve and modify various properties of the CuO film, such as adsorption, structure, sensitivity, and change in the band energy [46]. Bharathi et al. [47] formed a heterojunction between ZnO and CuO via the hydrothermal method. The sensor exhibited increased sensitivity due to the formation of a junction that can be considered a channel for gas reaction with nanocomposite. The grains acted as energetic sites for collecting gas. Chen et al. [48] explained the impact of doping on the CuO film. This study used Pt to dope the CuO film for detecting NO_2 gas using the dipping method. Pt-doped CuO has a thinner band gap and stronger contact with CuO, resulting in decreased resistance at 25 °C. The response changes more significantly as the temperature rises. This research suggested a feasible technique for creating high-performance, low-temperature NO_2 sensors for p-type CuO materials using several functionalization processes. Bo et al. [49] decorated a binary system (SnO_2/CuO) with rGO to detect NO_2 gas at room temperature. They found that the sensitivity to 50 ppm NO_2 gas was ~8–15× higher than that of CuO/rGO or SnO_2/rGO composites. In addition, the detection limit was 150 ppb, the stability was 7 d and good selectivity could be observed. These results were due to the contribution of the heterostructure of SnO_2/CuO nanoparticles.

GO

Graphene is a 2-D material considered promising and exciting in the current century due to numerous features such as high mobility, good conductivity, and a substantial specific surface area. GO is one of the graphene derivatives containing oxygen groups, making it more useful in gas sensors. GO can be synthesized from graphene using the traditional Hummers method [50]. As researchers report, rGO can be produced by thermal or chemical reduction of GO [51] and used in a lot of applications such as membranes [52], biomedical [53], bio-sensors [54], catalysts [55], energy storage devices [56], electronic devices [57], and light-emitting diodes [58]. In gas sensor applications, rGO achieved significant success because of their sensing properties, such as effective sites, increasing the interaction with target gas that enhances the sensor's sensitivity [59]. Kumar and Kaur [60] thermally reduced GO to generate rGO and obtained new characterizations for sensing. The response of this sensor was 3.3% for 5 ppm SO_2 gas at room temperature and appeared to have excellent selectivity. This is due to many defects in the sensor film that improve the sensor properties. Researchers reported that multilayer GO and rGO sensors can also be formed with other oxides to overcome the high operating temperature required for most oxides [61]. Majhi et al. [62] presented an overview and discussed the mechanism of rGO loaded with various oxide nanoparticles, for example, SnO_2, ZnO, CuO, In_2O_3, and Co_3O_4, in the gas sensing area. This study demonstrated that high surface area metal oxides loaded with rGO are the best option for sensing compared to rGO alone due to the long recovery and response time of rGO and low sensitivity. When rGO is loaded with other oxides, this leads to an increase in activation sites forming p-n or p-p junctions. The rGO/CuO multilayer was developed by Pisarkiewicz et al. [63] and selected for detecting NO_2 gas. Because the two oxides have distinct work functions, the electrons from CuO migrate towards rGO and holes from the latter to CuO, causing increased hole concentration, increasing conductivity, and confirming the sensor's sensitivity. Song et al. [64] used a mixing process to prepare a 4 nm diameter SnO_2 quantum wire

and place it onto a thin layer of GO. The sensor response was 17.9 when exposed to 10 ppm H_2S gas at 70 °C. This response was found to be superior to that of pure SnO_2, which worked at a higher temperature of 90 °C. Additionally, pure GO showed no response to H_2S gas. The enhancement of this sensor was primarily motivated by the superior electron transport capabilities exhibited by GO with less resistance. Pakdel et al. [65] used binary rGO-ZnO to develop the graphene-based sensor. This sensor exhibited superior sensitivity and selectivity towards 100 ppm NO_2 gas at 350 °C. The electron affinity of sensor materials and bond dissociation energy were credited with their remarkable selectivity to NO_2 when compared to bare ZnO and CuO.

ZnO

ZnO is an n-type semiconductor because it contains defects such as oxygen vacancies. The band gap of ZnO is around 3.37 eV and can be in various structures such as 0-D, 1-D, 2-D, and 3-D, but 1-D is more interesting for gas sensor applications. Low cost, thermal and chemical stability [66], and high conductivity are among the properties of ZnO and make detection more attractive [67-68]. Moreover, ZnO can form a heterojunction with other oxides by incorporating CuO with ZnO [69]. This study showed that CuO sensing toward NO_2 gas can be improved by creating a heterojunction with ZnO. The results were consistent with previous studies and the sensitivity of CuO/ZnO was greater than that of CuO due to a reduction in the depletion region of the p-n junction, resulting in a drop in conductivity. In contrast, the detection sensitivity towards NH_3 and CO gases exhibited a comparatively diminished response compared to NO_2 [70]. The characteristics of this sensor in humid and dry air for CO gas sensors were investigated at 100–450 °C. It was found that ZnO loses its selectivity in a humid environment but becomes highly selective for CO gas when doped with a small amount of Pd. When Pd was added to ZnO, the distinct work functions shown by metal and oxide materials created the Schottky transition barrier. Consequently, resistance was reduced when the barrier layer's thickness increased.

WO_3

WO_3 is a remarkable material for gas sensor and solar cell applications with a band gap of around 2.5–3.0 eV. It is an n-type semiconductor that can change its properties through doping and loading [71]. WO_3 shows good performance and fast response in gas sensors, it can be synthesized in various ways. WO_3 is found in numerous structures, such as nanofilms, nanotubes, and nanospheres. However, because of their natural structure and ease of fabrication, 1-D nanostructures are mostly utilized in gas sensors [72]. However, like any oxide, some drawbacks of WO_3 include limited selectivity and the requirement for high operating temperatures. Therefore, there is a need to develop the performance of sensing through the formation of phytocompounds with other oxides, such as GO, with different concentrations by hydrothermal method [73]. At an operating temperature of 150 °C and a concentration of 50 ppm acetylene gas, a response of around 15 was observed when 1 wt.% GO was added. The increased sensing qualities corresponded to the formed ohmic heterojunction and the synergistic effect of WO_3 and GO. The interaction between acetylene gas and oxygen ions led to a widening of the barrier layer, thereby increasing the response. Nakate et al. [74] mixed NiO with WO_3 in different ratios to synthesize an acetaldehyde gas sensor. The operating temperature for this sensor was 250 °C. It turned out that the response of this sensor was good. This is due to the formation of a junction between NiO and WO_3. The analytical gas adsorbs to the sensor surface and reacts with oxygen ions. Subsequently, electrons were released and combined with holes of NiO, reducing holes and expanding the depletion layer of NiO/WO_3. Therefore, resistance increases, which helps improve sensor response. Furthermore, WO_3 can be coated with SnO_2 nanoparticles by the sputtering method [75] for the H_2S gas sensor synthesis. The study revealed that the sensitivity of 1 ppm H_2S at 200 °C was 177 and appropriate selectivity for NH_3, NO_2, CO, and H_2 gases was achieved. The core (SnO_2) – shell (WO_3) structure was the key reason for the excellent selectivity

of the sensor, with the best thickness of WO_3 around 5 nm. WO_3 can also be doped with another metal [76]. For example, Adilakshmi et al. [77] used Ag nanoparticles to functionalize the WO_3 sensor via beam evaporation on a glass substrate. The results showed that the optimal Ag doping percentage of WO_3 to achieve 65 sensitivities to ethanol gas at 300 °C was 15 wt.% Ag, in addition to good stability and selectivity. A comparison of pure WO_3 and doped WO_3 was carried out and showed that the response was better when doping WO_3 than undoing. This is because of the introduced Ag nanoparticles, which cause a reduction in the barrier layer. Therefore, the response of the sensor improved. A comparison between different oxide gas sensors according to their response or sensitivity to different gases is given in Table 1.

■ THE MOS'S MECHANISM IN THE GAS SENSOR

The alteration in electrical conductivity of sensor films represents the essential principle of MOS gas sensors when exposed to the gas. This can be achieved through the interaction between metal oxides and test gas [87]. Fig. 3 shows the mechanism of the MOS gas sensor. When the surface of metal oxides is exposed to oxygen, their active sites absorb oxygen and form oxygen ions. This process is related to some indicators such as gas concentration, sensor film, temperature, and absorbed oxygen ions [88]. In addition, the type of semiconductor used is critical in detection. Regarding n-type semiconductors, the free electrons of the sensor film were reduced and accordingly, the resistance was increased. This interaction is expressed by the following Eq. (1–4) [89].

$$O_2(ads) + e^- \rightarrow O_2(ads) \quad (1)$$

$$O^-(ads) + e^- \rightarrow O^-(ads) \quad (2)$$

$$O_2^-(ads) + e^- \rightarrow 2O^-(ads) \quad (3)$$

$$O^-(ads) + e^- \rightarrow O^{2-}(ads) \quad (4)$$

Table 1. Different oxide gas sensors and their response to various gases

Material	Temperature (°C)	Response/Selectivity (%)	Gas	Ref.
CuO/GO	RT.	60.00	CO_2	[78]
WO_3	160	26.52	Ethanol	[79]
ZnO	150	15.00	H_2S	[80]
Go/SnO_2/NiO	350	21.11	Acetone	[81]
TiO_2	400	21.60	Acetone	[82]
ZnO/SnO_2	400	108.00	Ethanol	[83]
SnO_2	230	133.50	HCHO	[84]
CuO	400	90.00	NO_2	[85]
rCO	RT.	37.00	CO_2	[86]

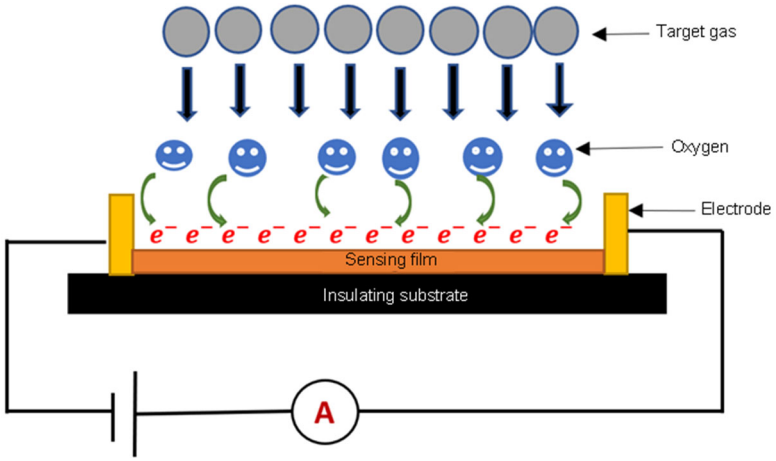

Fig 3. Mechanism of MOS gas sensor

However, for a p-type semiconductor, this resulted in an increase in conductivity due to excessive carrier concentration [90]. The interpretation of the exposure of the sensors to target gases was carried out according to the theory of the electron depletion layer/hole accumulation layer. When the n-type semiconductor is subjected to gas, electrons return to the MOS surface. As a consequence of this process, the barrier layer narrows, and the resistance decreases [91]. Holes represent the main carriers in a p-type semiconductor. When the gas flows across the MOS surface, electrons return to the surface, decreasing the accumulation layer and restoring the sensor's resistance [31].

■ SYNTHESIS OF MOS

The fabrication and synthesis of nanostructured metal oxide may be achieved using chemical or physical processes, as seen in Fig. 4. Chemical methods include the sol-gel process, polyol process, hydrothermal process, chemical vapor deposition (CVD), etc. Furthermore, physical methods include electron beam evaporation, milling, laser ablation, sputtering, etc. [92]. In this section, some of the synthesis methods will be introduced.

Sol-gel Method

Sol-gel is a bottom-up chemical process synthesizing metal oxides at low temperatures. It is distinguished by the control of both the dimensions and morphology of nanoparticles [93]. This process can be done in two steps. First, sol is formed from homogeneous molecules with the help of water or organic solvents [94]. After some chemical reactions, the sol becomes a denser, heavier, and more complex structure called a gel [95]. The gel formed has a structure with different properties and structure. The final and important step in sol-gel synthesis is thermal treatment to extract sediment and water molecules from the prepared sample and control the density and pore size of the material [96].

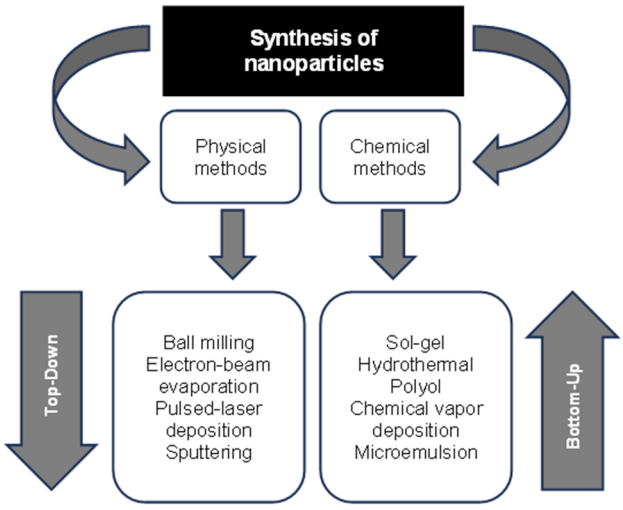

Fig 4. Methods of nanoparticle synthesis

Many researchers have adopted a simple sol-gel method in their work on synthesizing metal oxides. Shaposhnik et al. [97] used sol-gel synthesis to obtain SnO_2 gel from powders with a grain size of 5 nm. In addition to low cost and simplicity, this study demonstrated that the sensor sensitivity fabricated by this method was good for NH_3 gas with different concentrations. Patel et al. [98] prepared CuO and ZnO from copper nitrate and zinc nitrate by a sol-gel process. It was concluded from XRD results that the sizes of ZnO and CuO were about 61.25 and 21.82 nm, respectively. The SEM image results showed the good agglomeration of the CuO nanoparticles and illustrated the spherical shape of ZnO. Han et al. [99] decorated CuO nanowires with ZnO nanoparticles using different sol-gel concentrations. The length and width of NWs were 10–25 μm and 300–600 nm, respectively. The results of FESEM show that ZnO particles adhere to the surface of the CuO nanowires at different concentrations and that an additional concentration of sol-gel solution can destroy the structure of the CuO nanowires (Fig. 5(a-d)). The response of CuO/ZnO gas sensors was also investigated. The results demonstrated a better response toward 100 ppm NO_2 gas at 250 °C than the pristine CuO gas sensor had observed. In addition, rapid response and recovery times were observed. The response of 0.05 M CuO/ZnO was 4.1, which is higher than the response of pristine CuO. This improvement in sensor response at this concentration was due to the reduction in the width of the hall accumulation layers, which caused an increase in the sensor resistance (Fig. 5(e)).

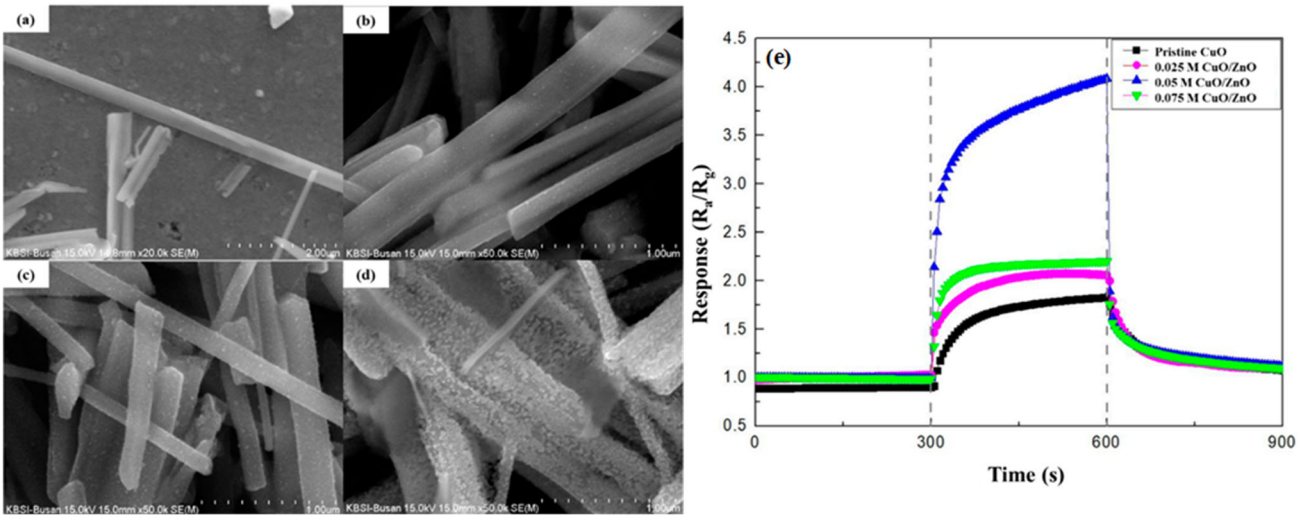

Fig 5. FESEM images and sensitivity of CuO and CuO/ZnO nanoparticles: (a) pristine CuO, (b) CuO nanowires decorated 0.025 M ZnO nanoparticles, (c) CuO nanowires decorated 0.050 M ZnO nanoparticles, (d) CuO nanowires decorated 0.075 M ZnO nanoparticles, and (e) dynamic response of pristine CuO and CuO nanowires decorated with different concentrations of ZnO nanoparticles toward NO_2 gas [99]

Hydrothermal Method

Hydrothermal is an easy synthesis method used to develop nanomaterials within the temperature range, including ambient temperature and a broad range of temperatures [100]. In this process, the reactants are dissolved in an aqueous medium in a closed system until they reach a heterogeneous reaction under high pressure [101]. Hydrothermal is usually used to produce nanospheres, nanowires, nanosheets, and nanorods [102]. Many research groups rely on this method to produce MOS. For example, WO_3 nanorods were synthesized from ammonium tungstate using this method.

On the other hand, San et al. [103] used a hydrothermal process to prepare rGO/In_2O_3 for the acetone gas sensor. At a concentration of 10 ppm acetone gas, a response was found at 5.6 at 150 °C. The good response and excellent stability at relatively low temperatures are due to the p-n heterojunction formed and the flower-like structure produced by this method. Sakthivel and Nammalvar [104] fabricated CuO/rGO nanostructure from copper nitrite and GO by hydrothermal technique. In this work, the reduction of GO and CuO was directly generated in one step at different preparation temperatures. As shown from the SEM and XRD results, the nanorod structure and cubic Cu_2O phase with an average diameter of 34 nm at 100 °C were observed. However, when the temperature was raised to 180 and 200 °C, the flower-like structure was formed, and the CuO phase was detected. The sensor response was ~14 to 600 ppm NH_3 at 200 °C. This increase in response was because of the large surface area of rGO, which determines the electrons on the CuO surface, which changed the sensor resistance**.** Claros and his groups [105] illustrated the impact of annealing temperature on the stabilization of nanostructures prepared by hydrothermal processes. They used copper acetate salt to produce CuO with a 50–200 nm diameter. It was shown that the sample annealed at 205 °C had no difference from the sample in the as-synthesized state. On the other hand, a sample annealed at 450 °C showed nanocrystals with a rough surface of 10–40 nm diameter. CuO nanowires showed excellent selectivity and high response to acetone gas and were independent of annealing temperature. The hydrothermal process was described by Zhang et al. [106] and appeared to be a successful synthesis of CuO nanoparticles in the 10 nm range. The SEM imaging results showed that there were more active-sites on the surface of the composites, which facilitated the hydrogenation process. Huang et al. [107] successfully prepared polypyrrole-coated cuprous

(PPy/Cu_2O) using a hydrothermal method at different temperatures and combined it with rGO. The as-prepared nanocomposites showed good sensitivity, repeatability, reversibility, and selectivity for NO_2 gas. The results of SEM displayed that the content of graphene has a great influence on the morphology of the nanocomposites, as shown in Fig. 6. The excessive amount of graphene may cause the stacking of graphene sheets and reduce the exposure of PPy-Cu_2O nanowires and the result in uneven dispersion, which is highly undesirable for gas sensing. The ratio of 0.1 composites achieved a maximum response of about 42.5 toward 50.0 ppm gas (Fig. 6(g)). A high response of 400%, a long stability of about 30 d, and a rapid response time of 6.8 s at very low temperatures of 23 °C were developed by Bai and colleagues [108]. This sensor was based on rGO@CuO, fabricated by a simple hydrothermal method to detect NO_2 gas. These good results were due to the cohesive effect between the two oxides. Porous found on the surface of CuO, high mobility of rGO carriers, and large surface area - all these indications increased the adsorption of active-sites for the gas, accelerated the surface reaction of nanocomposites, and then improved the sensing properties.

Pulsed Laser Deposition Method

The pulsed laser deposition (PLD) method is a top-down physical technique used to create nanostructures. In this method, a pulsed laser beam is directed toward the substrate, and the ablation process can form nanoparticles [109]. The interaction between laser and substrate strongly depends on factors such as pulse duration, wavelength, irradiance, and repetition rate. All of these parameters can influence the geometry and morphology of the sample [110]. This technique can produce various nanomaterials, such as ceramics, carbon nanomaterials, metal nanoparticles, and oxide composites [111]. There are numerous reasons for using a PLD, the most important of which is that a PLD can readily generate the energy necessary for a material to convert into plasma. Equally important is the laser's operating wavelength; thin film growth can be done at many wavelengths, although most thin film growth is done between 200–400 nm laser wavelengths when considering a laser for PLD. The basic reason for choosing these wavelengths is that most of the materials utilized for PLD have substantial absorption in these regions [112]. The main advantages of this technique are the capacity to regulate only laser energy density and pulse repetition rate during deposition, the ability to sequentially ablate targets to create multi-layered films of diverse materials, and the ability to control film thickness to atomic monolayer by number of pulses. One limitation of PLD is its relatively low average deposition rate and cost to apply thin layers of material. Challenges associated with the equipment setup include its complexity, limited compatibility with different

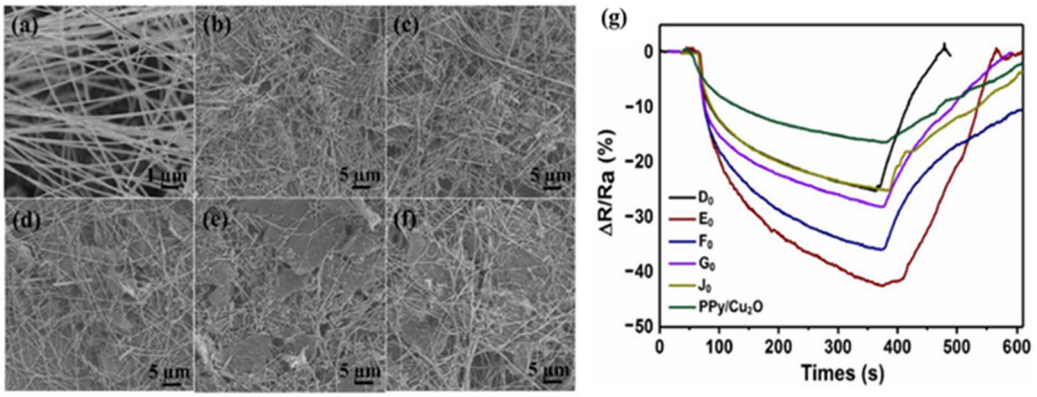

Fig 6. SEM image and gas sensor response of (a) PPy-Cu_2O nanowires prepared at 120 °C, and as-prepared rGO/PPy/Cu_2O nanocomposites after high-temperature thermal reduction with different mass ratio of GO (b) 0.08, (c) 0.10, (d) 0.12, (e) 0.15, (f) 0.20, and (g) gas sensing response curves of rGO/PPy/Cu_2O nanocomposites with different mass ratios of GO to 50 ppm NO_2 gas (D_0:0.08, E_0: 0.10, F0:$_0$.12, G_0:0.15, and J_0: 0.20) [107]

materials, high energy consumption, lack of uniformity, and sensitivity to substrate temperature [113].

Fadhil et al. [114] used Nd:YAG laser with a wavelength of 532 nm and repetition rate 1 Hz for the ablation of WO_3 pellets on glass and silicon substrates at 400 °C. The number of pulses was 100 pulses and laser fluence was 1.6 J/cm^2. The sensitivity of this sensor was recorded at room temperature and was 80% towards 3 ppm NO_2 gas. Another study conducted by Khudiar [115] used the same laser for preparing ZnO thin films but with a 1064 nm wavelength and repetition rate of 10 Hz. The energy of this laser ranged between 1.70 and 7.13 J/cm^2. Excellent H_2 gas sensitivity was recorded at an energy of 3.12 J/cm^2. The results showed that the sensing properties were enhanced when the grain size was above 20 nm.

Ball Milling Method

Ball milling is an effective top-down synthesis method for producing nanoparticles and amorphous materials from bulk materials at room temperature [116]. Generally, the ball mill consists of cylindrical (usually hollow) balls consisting of several ceramic, rubber or stainless-steel balls rotating around themselves [117]. Size, ball distribution, weight and shape have a crucial impact on grinding efficiency. The milling method is the basic principle of ball milling, in which nanotubes are ground into very small particles (powder) through the collision between the rigid balls, which creates high pressure [118]. Particle sizes up to 5 nm can be produced using mills with very high energy and critical speed [119-120]. Zhang et al. [121] prepared GO for NO_2 gas sensors by high-energy ball milling in a humid environment at room temperature. This low-cost gas sensor demonstrated excellent selectivity for NH_3 and NO_2 gas at concentrations as low as 25 ppm. Sapkota et al. [122] studied the effect of milling parameters on the ZnO thin film sensor. It was found that high porosity and tunable particle sizes can be obtained by changing the time or milling speed. Good response was found for sensors milled at 400 rpm and for 30 min in deionized water and ethylene glycol, which related to a high film porosity and enhanced variation in electron concentration resulting from adsorption/desorption of oxygen ions on the surfaces of ZnO nanoparticles. This improvement in sensor response was increased as the temperature was increased to 150 °C.

■ REDUCED AND OXIDIZED GASES - INTERACTION MECHANISM WITH MOS

Reduced Gases

Reducing gases like H_2S, NH_3, H_2, C_2H_5OH, and CO release electrons as they pass through the surface of the metal oxide due to the interaction between gases and desorbing oxygen ions on the surface of the metal. As a result, the density of the carrier charges changes, which alters the conductivity of the sensor layer [123].

H_2S

H_2S is a colorless and flammable gas. It has the odor of a rotting egg. The concentrations that humans can smell in the air are between 0.0005 and 0.3000 ppm. Concentrations above 20 ppm can irritate the upper respiratory tract [124]. H_2S has been found naturally in the breakdown of animals, humans, and bacteria and also found in natural gas and petroleum. The presence of H_2S and metal oxides at the surface may lead to a significant interaction between H_2S and the oxygen ions that are adsorbed, resulting in the production of SO_2 and the release of electrons which enhances the conductivity according to Eq. (5) [125]:

$$2H_2S + 3O_2^-(ads) \rightarrow 2H_2O + 2SO_2 + 3e^- \quad (5)$$

Researchers have reported various methods and materials for detecting H_2S gas. Park et al. [126] fabricated SnO_2/CuO nanofibers for detecting H_2S gas using electrospinning. The response for this sensor was 1395 at 200 °C. The porous SnO_2/CuO hollow nanofiber gas sensor has proven to be a potential choice for gas sensor systems due to enhanced surface area. On the other hand, Kim et al. [127] prepared p-p junctions from CuO-loaded rGO with different concentrations via electrospinning. The results showed the presence of numerous CuO-related nanograins in addition to p-p heterojunctions that can alternate when CuO is converted into CuS. This conversion from semiconducting to metallic type can lead to a strong

reaction of H_2S gas at 300 °C. Shujah et al. [128] fabricated an H_2S gas sensor using WO_3 as the sensing film using CVD method at different deposition temperatures. The experimental results showed that, in addition to high stability, this sensor also exhibited good response behavior for 10 ppm gas at 250 °C. This is owing to the interaction of H_2S gas with oxygen ions on the surface of WO_3, which causes electrons to be released and conductivity to rise.

CO

CO is a non-irritable gas, colorless and odorless, and light compared to air. The incomplete combustion of most organic compounds is the main source of CO gas [129]. However, CO can be emitted from fires, vehicle exhaust, smoke, and heating systems. CO is a reducing gas that combines with oxygen ions absorbed on the surface of the metal oxide, resulting in an excess of electrons on the oxide's surface. This reaction is represented in the following Eq. (6) and (7) [130].

$$2CO + O_2^-(ads) \rightarrow 2CO_2 + e^- \quad (6)$$

$$CO + O^-(ads) \rightarrow CO_2 + e^- \quad (7)$$

The oxidation process improves conductivity in an n-type semiconductor while reducing it in a p-type semiconductor [131]. Hjiri [132] reported a ZnO gas sensor at room temperature via the sol-gel method. Sensitivity was found to be 74% for 80 ppm with a rapid response time of 21 s. The reaction between the analytic gas and absorbed oxygen ions leads to a reduction in the depletion region and changed conductivity. Basu et al. [133] presented a cost-effective approach for creating α-Fe_2O_3 nanoparticles embedded in rGO sheets. These nanoparticles showed promise for sensitive 10 ppm CO gas detection at room temperature compared to pure α-Fe_2O_3 and rGO sheets due to their large surface area (19.047 m^2/g rGO-α-Fe_2O_3), rapid response (21 s) and recovery time (8 s). At room temperature, the material exhibits p-type semiconductivity and has a strong selectivity for CO gas alone. Molavi et al. [134] prepared pure and Al-doped CuO using the precipitation method for different concentrations of CO gas sensors. The results showed that Al enhanced the response of CuO due to the increase of surface area of CuO nanostructures for adsorption of gas molecules and high response. It was found that the response to 800 ppm CO for Al-doped CuO was about 20% larger than the response for pure CuO nanostructures. Dhage et al. [135] synthesized SnO_2-CuO for CO sensors using the precipitation method. The XRD results revealed that the nanocomposites had a good structure and high crystallinity and formation of SnO_2-CuO heterostructure, resulting in a response of 3.53 for 100 ppm CO gas at 200 °C. This enhancement in sensor responsiveness is due to the nanocomposite's increased surface area and heterojunction formation, leading to an increase in absorbed oxygen ions.

H_2

H_2 is a very light gas in nature. It is an odorless, tasteless, colorless, and flammable gas. In general, H_2 can be considered a non-toxic gas and represents about 70% of the mass of the universe around us. H_2 is deposited on the sensor film's surface, where it interacts with adsorbed oxygen to release electrons into the conduction band [136]. This increases the conductivity of the sensor layer at n-type and decreases its resistivity at p-type according to the Eq. 8 [137].

$$H_2 + O^-(ads) \rightarrow H_2O + e^- \quad (8)$$

Many researchers used H_2 gas sensors, Lu et al. [138] manufactured selective H_2 gas sensors using SnO_2 nanowires by a Solvothermal approach. The SnO_2 composite was applied to an Al_2O_3 substrate and annealed at 350 °C. The best response for 40 ppm H_2 gas was 13 at 250 °C with 15 s and 31 s response and recovery times, respectively. Following the introduction of Pd doping, a notable reduction in the operating temperature to 150 °C was observed, accompanied by a significant decrease in both the recovery and reaction time. The introduction of Pd as a dopant in SnO_2 resulted in a modification of the adsorption energy of SnO_2 on H_2 gas. Consequently, H_2 molecules exhibited adsorption on the surface of SnO_2, acting as a donor surface. This resulted in a reduction in resistance and changed the sensor's response. On the other hand, Das et al. [139] reported highly sensitive H_2 gas sensors by combining rGO with ZnO prepared by the chemical bath deposition method. The response was about 586.93% for 100 ppm gas with fast response and

recovery time. This improvement in response is due to the high carrier mobility of rGO the connection between two oxides and the transition between semiconductor and metal in the H_2 atmosphere. Chang et al. [140] fabricated Pt doping WO_3-based H_2 sensors using the thermal evaporation method. It was found that Pt doping WO_3 showed a higher response of 1.41×10^6 at 200 °C toward 1 ppm gas compared with bare WO_3.

Oxidized Gases

Oxidized gases such as O_2, NO_2, and CO_2 can take negative charges from the metal-oxide surface. This operation changes the thickness of the depletion layer and reduces the conductivity [141].

NO_2

NO_2 is a hazardous gas that results from the burning of oil, coal, and gas. Also, NO_2 can be generated from the internal combustion machine of cars and may be dangerous to human health [142]. The chemical interaction between NO_2 gas and oxygen ions on the surface occurs as the Eq. (9) and (10) [143].

$$2NO + O_2 \rightarrow 2NO_2 \quad (9)$$

$$NO_2 + e^-(surf) \rightarrow NO_2^- \quad (10)$$

The NO_2 gas induces an increase in resistance in the (n-type) metal oxide due to the capture of electrons from the sensor film. Conversely, a decrease in resistance occurs in the p-type metal oxide [144-145]. A soft sol-gel approach was used to fabricate a very selective NO_2 gas sensor based on CuO-ZnO [69]. It was found that the sensitivity of this sensor towards the target gas was higher compared to that of the pure CuO and ZnO materials. This is because the formation of hetero-junctions between two oxides leads to growth in the resistance due to the reduction of the hole-accumulation layer. However, when NO_2 was introduced, the resistance dropped due to the interaction of NO_2 gas with the surface electrons of CuO, resulting in a decrease in the number of electrons and an increase in the concentration of holes, and as a result, the conductivity rose. So, Sivakumar et al. [146] fabricated a NO_2 sensor by modifying rGO with SnO_2 using a simple hydrothermal method. It was proved from this study that this sensor was more sensitive to NO_2 gas and the response for 100 ppm NO_2 was 88.9 at 250 °C. This modulation in resistance is attributed to the wide depletion layer that is produced due to electron extraction from the surface of the film when NO_2 gas passes through it.

According to the synergistic - effect of SnO_2-rGO, Wang et al. [147] prepared the same NO_2 sensor but in the sol-gel method. This sensor exhibited high sensitivity compared with pristine rGO and showed the impact of humidity on sensing properties. The experimental results indicate that humidity, even at a relative humidity of 70% and a temperature of 116 °C, has little influence on the dynamic response to different gas concentrations. This owed to a superhydrophobic feature of the nanocomposites that contributed to humidity insensitivity. Petrov et al. [148] fabricated ZnO–SnO_2 using pyrolysis method. According to the results, the response for 50 ppm NO_2 gas was 146 at 200 °C with 144 s of response time. This result can be interpreted as a dipole moment induced by a surface electric field when NO_2 gas passes above the sensing film which causes an increment in the interaction energy between absorbent – adsorbent, altering the sensor's resistivity.

CO_2

CO_2 is an odorless, colorless gas that results from breathing, burning, and decomposition of organic material which may harm human health in some concentrations [149]. CO_2 is an oxidizer that interacts with oxygen ions adsorbed on the surface of sensing oxide, and ions of carbonate can be formed at high temperatures. The reaction can be expressed in Eq. (11) [150-151].

$$2CO_2 + 2O^{2-} \rightarrow 2CO_3^{2-} \quad (11)$$

This interaction leads to enhancing the sensor resistance in n-type and decreasing it in p-type [152]. Lee et al. [153] fabricated a CO_2 sensor based on SnO_2@rGO at room-temperature by chemical-reduction method. This sensor was examined within a broad range of gas concentrations and showed good sensitivity at a low limit of detection. It was found that the sensor response was about 1.206% to 100 ppm of CO_2 gas which was greater than the response of pristine rGO. This is owing to the presence of extra active sites

on the thick film's surface, rGO's high conductivity, and the formation of p-n junctions. Kohale [154] fabricated SnO_2/CuO sensor by screen printing technique for different concentrations of CO_2 gas. It was proved that the response reached 1.3 toward 1098 ppm of CO_2 gas at room temperature. It was observed from the results that some of Cu^{2+} ions were present on the surface, which increased the oxygen vacancies' concentration due to heterojunctions. When the sensor is exposed to CO_2 gas, it will be adsorbed on the Cu^{2+} sites to form a bond with an unshared electron pair in oxygen and an empty orbital in Cu^{2+} and change the resistance as a result of the rearrangement of electron cloud. ZnO gas sensor was synthesized by Kanaparthi and Singh [155]. This sensor's good sensitivity at 100 °C was due to the large surface area of ZnO nanocomposites, which may be explained by the oxygen vacancies hypothesis. It was found that the sensor's conductivity decreased as the sensor was in an air environment. However, when exposed to CO_2 gas, the interaction between oxygen ions (O^{2-}, O^-) and gas resulted in electron emission back into the conduction band and decreased resistance.

O_2

O_2 is a tasteless, odorless, and colorless gas essential to all living things. It is absorbed by animals and converted into CO_2, which plants use as a source of carbon and free O_2 back into the atmosphere [156]. Among the oxidizing gases, O_2 predominates and reacts with metal oxide surfaces more quickly than the others [157]. Increasing the operating temperature improves the adsorption of O_2 on the sensor layer by trapping electrons e operating temperature improves the adsorption of O_2 on the sensor layer by trapping electrons. This reaction can be expressed by the Eq. (12) and (13). The resistance of the sensor is enhanced for n-type semiconductors and diminished for p-type semiconductors [158].

$$O_2(gas) + e^- \rightarrow O_2^{2-}(ads) \quad (12)$$

$$2O_2(gas) + 2e^- \rightarrow 2O_2^{2-}(ads) \quad (13)$$

Recently, Raju and Li [159] presented a comprehensive analysis of the semiconductor mechanism in gas sensors, with particular emphasis on the adsorption of oxygen on the surfaces of p-type and n-type semiconductors. In semiconductors with n-conductivity, such as SnO_2, O_2 molecules are first absorbed on the surface of the SnO_2 material. This increases the junction area, reducing the resistance by reducing the electron concentration there. However, electrons are recaptured by the sensor film after the analysis gas combines. conversely, for a p-type semiconductor such as CuO, resistance is observed to increase when the film is exposed to gas. The observed phenomenon can be attributed to the increased emitted electron density, which leads to the formation of electron-hole pairs within the accumulation layer and a subsequent decrease in hole density. The following table briefly lists the influence of the type of gas on the resistance of the sensor (Table 2).

Table 2. Gas type effect on the sensor's resistance for p-type and n-type materials

Type of gas	Semiconductor - type	Resistance
Reducing - gas	n-type	decrease
	p-type	increase
Oxidizing - gas	n-type	increase
	p-type	decrease

■ MOS-BASED HETEROJUNCTIONS FOR GAS SENSORS

One of the disadvantages of metal oxides is the limited selectivity between identical gases because these gases have the same resistance changes, leading to difficulties in detecting the correct gas. Another disadvantage of metal oxides is the drift of the baseline resistance. This makes them significantly less accessible to the reactive gas, in addition to high power consumption and poor sensitivity. All these factors lead to the study and improvement of sensors through the formation of heterojunctions [160]. A heterojunction refers to the boundary or interface that exists between two semiconductors that possess different properties. This means different band gaps, contacts, and Fermi levels. To achieve equilibrium at the Fermi level, the movement of holes and electrons occurs in opposite directions in the context of two metal semiconductors [161]. Heterojunctions can manifest in three distinct forms: an isotype heterojunction (p-n, n-p), isotype heterojunction (p-p, n-n) and metal-semiconductor

heterojunction [162]. Fig. 7 shows heterojunctions (p-n, n-n, and p-p).

An Isotype Heterojunction (p-n/n-p)

An isotype heterojunction is a composite structure consisting of two semiconductors, wherein a secondary phase (p-type) is combined with a primary phase semiconductor (n-type) to create a p-n heterojunction, or, conversely, to generate an n-p heterojunction [163]. According to the difference between Fermi energy levels, electrons flow from high to low energy and in the opposite direction, the holes move until equilibrium can be achieved [160]. An electric field is induced due to the oppositely charged n and p regions, and a depletion layer forms between the two semiconductors. The buildup potential allows charge carriers to flow across the junction. Therefore, resistance will increase in this region [164]. The Fermi level in an n-type region is higher than that of the p-type region and due to the bending of both sides of the energy level, a potential barrier and a space charge zone are created. The study conducted by Mathew et al. [165] examined the effects of a ZnO–CuO heterojunction on the sensitivity to ethanol gas. The researchers observed that the higher ratio of surface area/volume of the heterojunction led to enhanced sensitivity. Nakate et al. [74] integrated NiO with WO_3 for the acetaldehyde gas sensor. This sensor appeared to have a high response to the analysis gas. Zhang et al. [166] successfully prepared CuO-SnO_2 by changing the concentrations of two oxides and adjusting the type of solvent used in the hydrothermal method. The results of this study showed an excellent response to ethanol gas when deionized water was used as a solvent. The SEM and XDR analyses revealed a well-defined core-shell structure of the composite material. Specifically, when the molarity ratio of Cu:Sn=1:1 was used, the sensor response was significantly improved, reaching a value of 32.

Isotype Heterojunctions (n-n and p-p)

The heterojunction between the material itself (n-n or p-p) is called an isotype transition. As an isotype, the charge carrier (electrons or holes) is transferred to the lowest Fermi level [167]. This process resulted in the formation of a depletion layer or accumulation layer composed of either electrons or holes, which in turn promotes oxygen adsorption to the surface [168]. The principle of n-n heterojunction depends on the formation of the accumulation region as a result of electron conversion from the highest energy [31]. Many researchers reported improved gas detection performance based on n-n heterojunctions. Du et al. [169] presented a sensor array composed of ZnO and SnO_2. This preparation showed an increase in response with increased temperatures from 200 to 400 °C toward ethanol gas. Improved in sensor response might be due to adsorbed oxygen and more electron transfer between SnO_2/ZnO heterojunction and ethanol gas. Xue et al. [170] used WO_3·H_2O and SnO_2 as precursors to produce WO_3/SnO_2 sensors by simple impregnation and calcination. The study showed that nanocomposites exhibited both long-term stability and a favorable reaction to CH_4 gas. Specifically, the response of nanocomposites

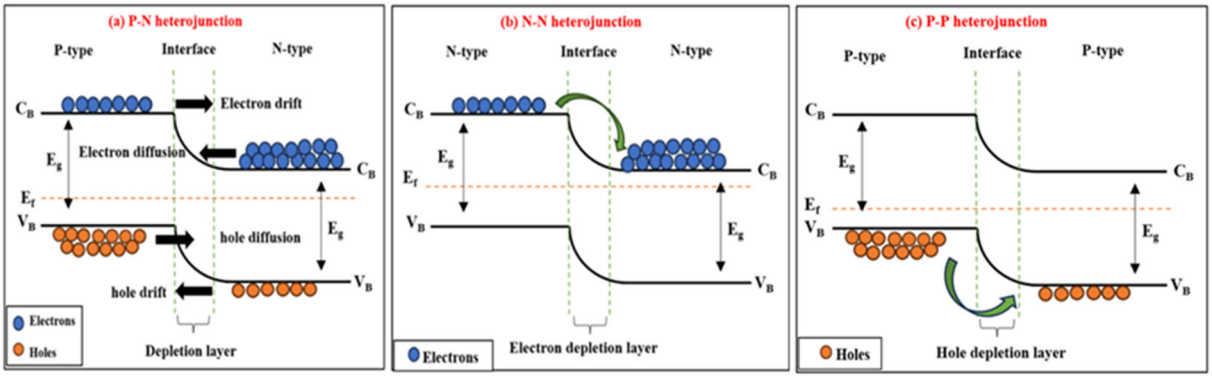

Fig 7. Schematic diagrams of the energy band structure at heterojunction interfaces of different types of heterojunctions: (a) p–n, (b) n–n, and (c) p–p

to CH_4 gas was roughly 1.4× greater compared to WO_3 alone. These observations were made at relatively moderate temperatures of around 90 °C. The refinement in response was related to the creation of an n-n junction, which resulted in an excess of defects and excessive surface area by SnO_2. For a p-p heterojunction, at the interface of two junctions, a hole accumulation layer and a hole depletion layer combine [171]. The holes are injected into the barrier layer by adsorbed oxygen ions. As a consequence, there is a decrease in the thickness of the barrier layer, resulting in a corresponding decrease in resistance [172]. Sarode et al. [173] used an ultrasound-assisted method to synthesize GO–CuO and its nanofluids from copper nitrate and disodium citrate with GO solution. This article is about studying the heat transfer properties of nanofluids. The results showed that thermal conductivity was proportional to temperature and increased with increasing concentration on (0.03 vol%) GO-CuO nanofluids. Conductivity was measured to be 1.046 W mK^{-1} at this concentration and temperature, while the heat transfer coefficient was measured to be 1474.99 Wm^{-2} K^{-1}. Recently, a water bath heating strategy was used to prepare rGO/CuO nanoparticles. The diameter and surface area were calculated to be 100.00 nm and 31.32 nm^2, respectively. Significant improvements in recovery and response times were observed, along with a significant sensitivity to formaldehyde gas of 49% at a temperature of 80 °C, compared to the pure CuO and rGO. These obtained results were due to the excellent sensing properties of the as-prepared nanocomposites and the good conductivity of rGO. In another study [174], a microwave-assisted technique was used to synthesize CuO/rGO nanoparticles. When exposed to 10 ppm of H_2S gas at a relatively moderate temperature of 100 °C, the sensor showed a favorable response of roughly 68.5. The presence of a heterojunction between two distinct materials, represented as p-p, could contribute to the increase in sensor response. The disparate work functions shown by the two oxides result in the migration of holes towards CuO, where they undergo recombination with electrons emitted by the H_2S gas. This process continues until the Fermi level attains equilibrium. As a result, there is a reduction in the concentration of holes and an elevation in resistance.

Metal-Semiconductor Heterojunction

Many metals are utilized to dope metal oxides through various synthesis techniques to alter the characterization of the sensors due to their chemical and electrical properties. Their metals include Pt, Au, Ag, Pd, etc. [175]. The heterojunction is an interface between metal oxide and metal. The difference between the electron concentration in metal/metal oxides motivates the conversion of electrons between two contacts until equilibrium occurs [176]. The formation of an Ohmic or Schottky contact was determined based on the metal's work function (ϕ_m) with the n-type semiconductor. In the case where the ϕ_m of the metal exceeds that of the oxide (ϕs), the transfer of electrons occurs from a semiconductor with a high Fermi level to the metal [177]. The process described leads to the accumulation of negative charges, namely electrons, on the surface of the metal, while positive charges, or holes, accumulate on the surface of the semiconductor. Bending the tape upward results in forming a Schottky barrier, which subsequently gives rise to a potential barrier [161]. When the ϕ_m is lower than ϕs, there is a migration of electrons from the metal to the semiconductor. As a result, the concentration of electrons on the surface of the semiconductor becomes greater than that in the bulk [178]. This creates a high conductivity and the ohmic contact is created. In p-type semiconductors, the ohmic contact occurs when ϕ_m is greater than ϕ_s, and the rectifier contact occurs when the opposite happens [179]. Ag is a very effective metal that enhances the sensing capabilities of TiO_2 by increasing the number of active sites for the adsorption of O_2 molecules. Additionally, the presence of Ag alters the response characteristics of the sensor. Kumar et al. [180] increased sensor gas performance by combining graphene and metal oxides owing to the synergistic impact of three-dimensional material and metal oxide. Another group used Ag to dope In_2O_3 with different concentrations through hydrothermal process to improve the NO_2 gas sensor at 100 °C [181]. The results of XRD and FESEM

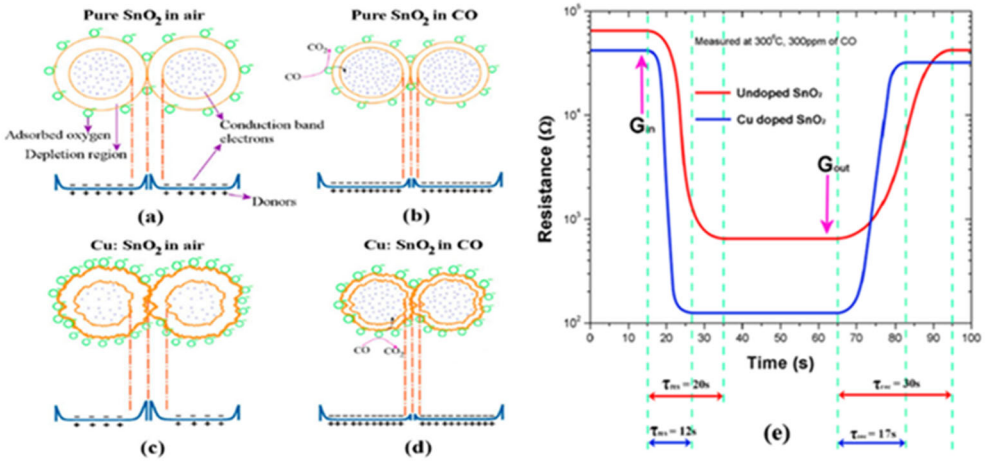

Fig 8. Gas sensor mechanism and sensitivity of the pure SnO_2 in (a) air and (b) CO; Cu-SnO_2 pellets in (c) air (d) CO; and (e) sensitivity, response, recovery times of pure SnO_2 and Cu-SnO_2 pellets [182]

showed high crystallinity of In_2O_3 and the size of this crystallite decreased with increasing Ag concentration. It was observed that 9% Ag achieved a sensitivity of about 79%, which was attributed to the enhancement of gas absorption on the metal oxide surface and then increased the sensitivity. Karthik et al. [182] used Cu in their study to incorporate SnO_2 for the fabrication of CO gas sensors. Fig. 8(a–d) below shows the principle of gas sensing in Cu-SnO_2 and pure SnO_2 powder. Fig. 8(e) demonstrates the response and recovery times for pure and Cu-SnO_2 pellets at 300 °C and 300 ppm CO gas concentration. Cu-SnO_2 has significantly decreased response and recovery times by a factor of two due to alteration in structural and morphological occurring to SnO_2 after incorporation with Cu resulting in increased sensitivity to 348.4 and shorter response and recovery times to about 10.8 and 15.3, respectively.

■ CONCLUSION

The MOS has been the focal point for developing efficient gas sensors due to their intrinsic characteristics. This review article provides the different types of MOS and recent progress in sensing mechanisms for detecting different kinds of hazardous and flammable gases, as well as different methods used to synthesize them. The strategies to the improvement of gas sensing have also been summarized. The study of MOS gas sensors suffers from a lot of challenges. Further studies and more experiments are needed to understand how different gas-detecting mechanisms affect the performance of sensors. Considering chemical and physical adsorption processes in MOS helps explain its selectivity for a certain gas. The desorption process on the MOS surface requires more energy to increase sensor speed. Evaluating the processes involved in the gas-sensitive process might improve our understanding of present tactics for improving sensitivity. Analyzing the mechanisms of gas sensing indicators might lead to new or improved strategies, balancing compromises in other aspects. MOS-based gas sensors can only achieve a better market value by enhancing their overall performance. Although research on MOS-based gas sensors is growing, many papers lack detailed information on gas detection.

■ ACKNOWLEDGMENTS

We thank the Department of Physics, College of Science, University of Kerbala, Kerbala, Iraq, for its assistance in accomplishing this work.

■ CONFLICT OF INTEREST

There are no pertinent financial or non-financial interests that the authors need to disclose.

■ AUTHOR CONTRIBUTIONS

All authors participate in writing this study. Inam Abed Hammod, Noor Jawad Ridha, Khawla Jemeel Tahir, Firas Kamel Mohamad Alosfur, Asaad Sabbar Yasir, and Luma Ahmed Majeed wrote the manuscript,

tables designed, drawing figures, and reviewed the manuscript. All contributors provided feedback on earlier drafts of the work, with Inam A. Hammod writing the original draft. All writers read and approved the completed work.

■ REFERENCES

[1] Mirzaei, A., Lee, J.H., Majhi, S.M., Weber, M., Bechelany, M., Kim, H.W., and Kim, S.S., 2019, Resistive gas sensors based on metal-oxide nanowires, *J. Appl. Phys.*, 126 (24), 241102.

[2] Hermawan, A., Septiani, N.L.W., Taufik, A., Yuliarto, B., Suyatman, S., and Yin, S., 2021, Advanced strategies to improve performances of molybdenum-based gas sensors, *Nano-Micro Lett.*, 13, 207.

[3] Ji, H., Zeng, W., and Li, Y., 2019, Gas sensing mechanisms of metal oxide semiconductors: A focus review, *Nanoscale*, 11 (47), 22664–22684.

[4] Liu, L., Wang, Y., Liu, Y., Wang, S., Li, T., Feng, S., Qin, S., and Zhang, T., 2022, Heteronanostructural metal oxide-based gas microsensors, *Microsyst. Nanoeng.*, 8 (1), 85.

[5] Wawrzyniak, J., 2023, Advancements in improving selectivity of metal oxide semiconductor gas sensors opening new perspectives for their application in food industry, *Sensors*, 23 (23), 9548.

[6] Chai, H., Zheng, Z., Liu, K., Xu, J., Wu, K., Luo, Y., Liao, H., Debliquy, M., and Zhang, C., 2022, Stability of metal oxide semiconductor gas sensors: A review, *IEEE Sens. J.*, 22 (6), 5470–5481.

[7] Lu, N., Fan, S., Zhao, Y., Yang, B., Hua, Z., and Wu, Y., 2021, A selective methane gas sensor with printed catalytic films as active filters, *Sens. Actuators, B*, 347, 130603.

[8] Liang, Y., Wu, C., Jiang, S., Jie , Y., Wu, D., Li, M., Cheng, P., Yang, W., Cheng, C., Li, L., Deng, T., Sun, J.Y., He, G., Liu, B., Yao, T., Wu, M., and Zhou, Z., 2021, Field comparison of electrochemical gas sensor data correction algorithms for ambient air measurements, *Sens. Actuators, B*, 327, 128897.

[9] Feng, W., Qu, Y., Gao, Y., and Ma, Y., 2021, Advances in fiber-based quartz enhanced photoacoustic spectroscopy for trace gas sensing, *Microwave Opt. Technol. Lett.*, 63 (8), 2031–2039.

[10] Zheng, Q., Zhang, H., Liu, J., Xiao, L., Ao, Y., and Li, M., 2021, High porosity fluorescent aerogel with new molecular probes for formaldehyde gas sensors, *Microporous Mesoporous Mater.*, 325, 111208.

[11] Amirjani, A., and Rahbarimehr, E., 2021, Recent advances in functionalization of plasmonic nanostructures for optical sensing, *Microchim. Acta*, 188 (2), 57.

[12] Amirjani, A., Salehi, K., and Sadrnezhaad, S.K., 2022, Simple SPR-based colorimetric sensor to differentiate Mg^{2+} and Ca^{2+} in aqueous solutions, *Spectrochim. Acta, Part A*, 268, 120692.

[13] Amirjani, A., Kamani, P., Hosseini, H.R.M., and Sadrnezhaad, S.K., 2022, SPR-based assay kit for rapid determination of Pb^{2+}, *Anal. Chim. Acta*, 1220, 340030.

[14] Shahsavandi, F., Amirjani, A., and Reza Madaah Hosseini, H., 2022, Plasmon-enhanced photocatalytic activity in the visible range using AgNPs/polydopamine/graphitic carbon nitride nanocomposite, *Appl. Surf. Sci.*, 585, 152728.

[15] Moumen, A., Kumarage, G., and Comini, E., 2022, P-type metal oxide semiconductor thin films: synthesis and chemical sensor applications, *Sensors*, 22 (4), 1359.

[16] Abdeslam, A.A., Fouad, K., and Khalifa, A., 2020, Design and optimization of platinium heaters for gas sensor, *Dig. J. Nanomater. Biostruct.*, 15 (1), 133–141.

[17] Hasan, M.N., Acharjee, D., Kumar, D., Kumar, A., and Maity, S., 2016, Simulation of low power heater for gas sensing application, *Procedia Comput. Sci.*, 92, 213–221.

[18] Yuan, Z., Li, R., Meng, F., Zhang, J., Zuo, K., and Han, E., 2019, Approaches to enhancing gas sensing properties: A review, *Sensors*, 19 (7), 1495.

[19] Alamri, M., Liu, B., Berrie, C.L, Walsh, M., and Wu, J.Z., 2022, Probing the role of CNTs in Pt nanoparticle/CNT/graphene nanohybrids H_2S sensors, *Nano Express*, 3 (3), 035004.

[20] Guan, W., Tang, N., He, K., Hu, X., Li, M., and Li, K., 2020, Gas-sensing performances of metal oxide nanostructures for detecting dissolved gases: A mini review, *Front. Chem.*, 8, 00076.

[21] Riente, P., and Noël, T., 2019, Application of metal oxide semiconductors in light-driven organic transformations, *Catal. Sci. Technol.*, 9 (19), 5186–5232.

[22] Li, B., Zhou, Q., Peng, S., and Liao, Y., 2020, Recent advances of SnO_2-based sensors for detecting volatile organic compounds, *Front. Chem.*, 8, 00321.

[23] Nalimova, S., Shomakhov, Z, and Moshnikov, V., 2023, Binary and ternary oxide nanostructured multisystems for gas sensors, *Eng. Proc.*, 48 (1), 47.

[24] Zhao, G., Xuan, J., Liu, X., Jia, F., Sun, Y., Sun, M., Yin, G., and Liu, B., 2019, Low-cost and high-performance ZnO nanoclusters gas sensor based on new-type FTO electrode for the low-concentration H_2S gas detection, *Nanomaterials*, 9 (3), 435.

[25] Khort, A., Haiduk, Y., Taratyn, I., Moskovskikh, D., Podbolotov, K., Usenka, A., Lapchuk, N., and Pankov, V., 2023, High-performance selective NO_2 gas sensor based on In_2O_3–graphene–Cu nanocomposites, *Sci. Rep.*, 13 (1), 7834.

[26] Lu, Z., Ma, Z., Song, P., and Wang, Q., 2021, Facile synthesis of CuO nanoribbons/rGO nanocomposites for high-performance formaldehyde gas sensor at low temperature, *J. Mater. Sci.: Mater. Electron.*, 32 (14), 19297–19308.

[27] Ren, Z., Shi Y., Song, T., Y., Wang, T., Tang, B., Niu, H., and Yu, X., 2021, Flexible low-temperature ammonia gas sensor based on reduced graphene oxide and molybdenum disulfide, *Chemosensors*, 9 (12), 345.

[28] Lei, G., Lou, C., Liu, X., Xie, J., Li, Z., Zheng, W., and Zhang, J., 2021, Thin films of tungsten oxide materials for advanced gas sensors, *Sens. Actuators, B*, 341, 129996.

[29] Kamble C., and Panse, M., 2019, IDE embedded tungsten trioxide gas sensor for sensitive NO_2 detection, *Mater. Chem. Phys.*, 224, 257–263.

[30] Saruhan, B., Lontio Fomekong, R., and Nahirniak, S., 2021, Review: Influences of semiconductor metal oxide properties on gas sensing characteristics, *Front. Sens.*, 2, 657931.

[31] Zhang, H., Guo, Y., and Meng, F., 2022, Metal oxide semiconductor sensors for triethylamine detection: Sensing performance and improvements, *Chemosensors*, 10 (6), 231.

[32] Zhang, D., Yang, Z., Yu, S., Mi, Q., and Pan, Q., 2020, Diversiform metal oxide-based hybrid nanostructures for gas sensing with versatile prospects, *Coord. Chem. Rev.*, 413, 213272.

[33] Suhendi, E., Amanda, Z.L., Ulhakim, M.T., Setiawan, A., and Syarif, D.G., 2021, The enhancement of ethanol gas sensors response based on calcium and zinc co-doped $LaFeO_3/Fe_2O_3$ thick film ceramics utilizing yarosite minerals extraction as Fe_2O_3 precursor, *J. Met., Mater. Miner.*, 31 (2), 71–77.

[34] Kadhim, H., Ahmed, L., and AL-Hachamii, M., 2022, Facile synthesis of spinel $CoCr_2O_4$ and its nanocomposite with ZrO_2: Employing in photo-catalytic decolorization of Fe (II)(luminol-tyrosine) complex, *Egypt. J. Chem.*, 65 (1), 481–488.

[35] Galstyan, V., Ponzoni, A., Kholmanov, I., Natile, M.M., Comini, E., and Sberveglieri, G., 2022, Highly sensitive and selective detection of dimethylamine through Nb-doping of TiO_2 nanotubes for potential use in seafood quality control, *Sens. Actuators, B*, 303, 127217.

[36] Jawad, T.M., AL-Lami, M.R., Hasan, A.S., Al-Hilifi, J.A., Mohammad, R.K., and Ahmed, L., 2021, Synergistic effect of dark and photoreactions on the removal and photo-decolorization of azo carmosine dye (E122) as food dye using rutile-TiO_2 suspension, *Egypt. J. Chem.*, 64 (9), 4857–4865.

[37] Nikolic, M.V., Milovanovic, V., Vasiljevic, Z.Z., and Stamenkovic, Z., 2020, Semiconductor gas sensors: Materials, technology, design, and application, *Sensors,* 20 (22), 6694.

[38] Aarti, A., Gaur, A., Chand, P., Shah, J., and Kotnala, R.K., 2022, Tin oxide (SnO_2)-decorated reduced graphene oxide (rGO)-based hydroelectric cells to generate large current, *ACS Omega*, 7 (48), 43647–43656.

[39] Annanouch, F.E., Bendahan, M., Bouchet, G., Perrier, P., Morati, N., Martini-Laithier, V., Fiorido, T., and Aguir, K., 2019, Optimized testing chamber for qualified sensor responses measurement, *Sens. Transducers*, 222 (6), 12–17.

[40] Chen, T., Sun, J., Xue, N., Wang, W., Luo, Z., Liang, Q., Zhou, T., Quan, H., Cai, H., Tang, K., and Jiang, K., 2023, Cu-doped SnO_2/rGO nanocomposites for ultrasensitive H_2S detection under low temperature, *Microsyst. Nanoeng.*, 9 (1), 69.

[41] Ayesh, A.I., Alyafei, A.A., Anjum, R.S., Mohamed, R.M., Abuharb, M.B., Salah, B., and El-Muraikhi, M., 2019, Production of sensitive gas sensors using CuO/SnO_2 nanoparticles, *Appl. Phys. A*, 125 (8), 550.

[42] Guo, J., Li, W., Zhao, X., Hu, H., Wang, M., Luo, Y., Xie, D., Zhang, Y., and Zhu, H., 2021, Highly sensitive, selective, flexible and scalable room-temperature NO_2 gas sensor based on hollow SnO_2/ZnO nanofibers, *Molecules*, 26 (21), 6475.

[43] Rodiawan, R., Wang, S.C., and Suhdi, S., 2023, Gold-nanoparticle-decorated tin oxide of a gas sensor material for detecting low concentrations of hydrogen sulfide, *Sens. Mater.*, 35 (3), 1121–1130.

[44] Steinhauer, S., 2021, Gas sensors based on copper oxide nanomaterials: A review, *Chemosensors*, 9 (3), 51.

[45] Peng, F., Sun, Y., Lu, Y., Yu, W., Ge, M., Shi, J., Cong, R., Hao, J., and Dai, N., 2020, Studies on sensing properties and mechanism of CuO nanoparticles to H_2S gas, *Nanomaterials*, 10 (4), 774.

[46] Hittini, W., Abu-Hani, A., Reddy, N., and Mahmoud, S.T., 2020, Cellulose-copper oxide hybrid nanocomposites membranes for H_2S gas detection at low temperatures, *Sci. Rep.*, 10 (1), 2940.

[47] Bharathi, P., Karthigeyan, S., and Krishna, M., 2022, Synthesis and functional properties of ZnO/CuO nanocomposite for gas sensing applications, *IOP Conf. Ser.: Mater. Sci. Eng.*, 1219 (1), 012053.

[48] Chen, X., Liu, T., Ouyang, Y., Huang, S., Zhang, Z., Liu, F., Qiu, L., Wang, C., Lin, X., Chen, J., and Shen, Y., 2024, Influence of different Pt functionalization modes on the properties of CuO gas-sensing materials, *Sensors*, 24 (1), 120.

[49] Bo, Z., Wei, X., Guo, X., Yang, H., Mao, S., Yan, J., and Cen, K., 2020, SnO_2 nanoparticles incorporated CuO nanopetals on graphene for high-performance room-temperature NO_2 sensor, *Chem. Phys. Lett.*, 750, 137485.

[50] Hummers Jr, W.S., and Offeman, R.E., 1958, Preparation of graphitic oxide, *J. Am. Chem. Soc.*, 80 (6), 1339.

[51] Imamura, G., Minami, K., Shiba, K., Mistry, K., Musselman, K.P., Yavuz, M., Yoshikawa, G., Saiki, K., and Obata, S., 2020, Graphene oxide as a sensing material for gas detection based on nanomechanical sensors in the static mode, *Chemosensors*, 8 (3), 82.

[52] Tiwary, S.K., Singh, M, Chavan, S.V., and Karim, A., 2024, Graphene oxide-based membranes for water desalination and purification, *npj 2D Mater. Appl.*, 8 (1), 27.

[53] Zare, P., Aleemardani, M., Seifalian, A., Bagher, Z., and Seifalian, A.M., 2021, Graphene oxide: Opportunities and challenges in biomedicine, *Nanomaterials*, 11 (5), 1083.

[54] Sethi, J., Van Bulck, M., Suhail, A., Safarzadeh, M., Perez-Castillo, A., and Pan, G., 2020, A label-free biosensor based on graphene and reduced graphene oxide dual-layer for electrochemical determination of beta-amyloid biomarkers, *Microchim. Acta*, 187 (5), 288.

[55] Sachdeva, H., 2020, Recent advances in the catalytic applications of GO/rGO for green organic synthesis, *Green Process. Synth.*, 9 (1), 515–537.

[56] Kumar, H., Sharma, R., Yadav, A., and Kumari, R., 2021, Recent advancement made in the field of reduced graphene oxide-based nanocomposites used in the energy storage devices: A review, *J. Energy Storage*, 33, 102032.

[57] Wu, J., Lin, H., Moss, D.J., Loh, K.P., and Jia, B., 2023, Graphene oxide for photonics, electronics and optoelectronics, *Nat. Rev. Chem.*, 7 (3), 162–183.

[58] Song, S.H., Yoo, J.I., Kim, H.B., Kim, Y.S., So Kim, S., and Song, J.K., 2022, Hole injection improvement in quantum-dot light-emitting diodes using bi-layered hole injection layer of

PEDOT:PSS and V_2O_x, *Opt. Laser Technol.*, 149, 107864.

[59] Lun, D., and Xu, K., 2022, Recent progress in gas sensor based on nanomaterials, *Micromachines*, 13 (6), 919.

[60] Khune, A.S., Padghan, V., Bongane, R., Narwade, V.N., Dole, B.N., Ingle, N.N., Tsai, M.L., Hianik, T., and Shirsat, M.D., 2023, Highly selective chemiresistive SO_2 sensor based on a reduced graphene oxide/porphyrin (rGO/TAPP) composite, *J. Electron. Mater.*, 52 (12), 8108–8123.

[61] Smith, A.T., LaChance, A.M., Zeng, S., Liu, B., and Sun, L., 2019, Synthesis, properties, and applications of graphene oxide/reduced graphene oxide and their nanocomposites, *Nano Mater. Sci.*, 1 (1), 31–47.

[62] Majhi, S.M., Mirzaei, A., Kim, H.W., and Kim, S.S., 2021, Reduced graphene oxide (rGO)-loaded metal-oxide nanofiber gas sensors: An overview, *Sensors*, 21 (4), 1352.

[63] Pisarkiewicz, T., Maziarz, W., Małolepszy, A., Stobiński, L., Michoń, D., and Rydosz, A., 2020, Multilayer structure of reduced graphene oxide and copper oxide as a gas sensor, *Coatings*, 10 (11), 1015.

[64] Song, Z., Yan, J., Lian, J., Pu, W., Jing, L., Xu, H., and Li., H., 2020, Graphene oxide-loaded SnO_2 quantum wires with sub-4 nanometer diameters for low-temperature H_2S gas sensing, *ACS Appl. Nano Mater.*, 3 (7), 6385–6393.

[65] Pakdel, H., Borsi, M., Ponzoni, M., and Comini, E., 2024, Enhanced gas sensing performance of CuO-ZnO composite nanostructures for low-concentration NO_2 detection, *Chemosensors*, 12 (4), 54.

[66] Hussain, Z.A., Fakhri, F.H., Alesary, H.F., and Ahmed, L.M., 2020, ZnO based material as photocatalyst for treating the textile anthraquinone ZnO based material as photocatalyst for treating the textile anthraquinone derivative dye (dispersive blue 26 dye): Removal and photocatalytic treatment, *J. Phys.: Conf. Ser.*, 1664 (1), 1–15.

[67] Yu, S., Chen, C. Zhang, H., Zhang, J., and Liu, J., 2021, Design of high sensitivity graphite carbon nitride/zinc oxide humidity sensor for breath detection, *Sens. Actuators, B*, 332, 129536.

[68] Martínez-Pacheco, C., Cervantes-López, J.L., López-Guemez, A.R., López-Rodríguez, A.S., Sifuentes-Gallardo, P., Díaz-Guillen, J.C., and Díaz-Flores, L.L., 2024, Preparation of ZnO thick films activated with UV-LED for efficient H_2S gas sensing, *Coatings*, 14 (6), 693.

[69] Navale, Y.H., Navale, S.T., Stadler, F.J., Ramgir, N.S., and Patil, V.B., 2019, Enhanced NO_2 sensing aptness of ZnO nanowire/CuO nanoparticle heterostructure-based gas sensors, *Ceram. Int.*, 45 (2, Part A), 1513–1522.

[70] Platonov, V., Rumyantseva, M., Khmelevsky, N., and Gaskov, A., 2020, Electrospun ZnO/Pd nanofibers: CO sensing and humidity effect, *Sensors,* 20 (24), 7333.

[71] Dong, C., Zhao, R., Yao, L., Ran, Y., Zhang, X., and Wang, Y., 2020, A review on WO_3 based gas sensors: Morphology control and enhanced sensing properties, *J. Alloys Compd.*, 820, 153194.

[72] Nakate, U.T., Singh, V.K., Yu, Y.T., and Park, S., 2021, WO_3 nanorods structures for high-performance gas sensing application, *Mater. Lett.*, 299, 130092.

[73] Li, X., Fu, L., Karimi-Maleh, H., Chen, F., and Zhao, S., 2024, Innovations in WO_3 gas sensors: Nanostructure engineering, functionalization, and future perspectives, *Heliyon*, 10 (6), e27740.

[74] Nakate, U.T., Yu, Y.T., and Park, S., 2021, High performance acetaldehyde gas sensor based on p-n heterojunction interface of NiO nanosheets and WO_3 nanorods, *Sens. Actuators, B*, 344, 130264.

[75] Hoa, T.T.N., Le, D.T.T., Van Toan, N., Van Duy, N., Hung, C.M., Van Hieu, N., and Hoa, N.D., 2021, Highly selective H_2S gas sensor based on WO_3-coated SnO_2 nanowires, *Mater. Today Commun.*, 26, 102094.

[76] He, Y., Shi, X., Chen, K., Yang, X., and Chen, J., 2020, Titanium-doped p-type WO_3 thin films for liquefied petroleum gas detection, *Nanomaterials*, 10 (4), 747.

[77] Adilakshmi, G., Reddy, R.S., Reddy, A.S., Reddy, P.S., and Reddy, C.S., 2020, Ag-doped WO_3 nanostructure films for organic volatile gas sensor

application, *J. Mater. Sci.: Mater. Electron.*, 31 (15), 12158–12168.

[78] Bhat, N., Ukkund, S.J., Ashraf, M., Acharya, K., Ramegouda, N.J., Puthiyillam, P., Hasan, M.A., Islam, S., Koradoor, V.B., Praveen, A.D., and Khan, M.A., 2023, GO/CuO nanohybrid-based carbon dioxide gas sensors with an Arduino detection unit, *ACS Omega*, 8 (36), 32512–32519.

[79] Xiao, J., Che, Y., Lv, B., Benedicte, M.C., Feng, G., Sun, T., and Song, C., 2021, Synthesis of WO_3 nanorods and their excellent ethanol gas-sensing performance, *Mater. Res.*, 24 (3), e20200434.

[80] Onkar, S.G., Nagdeote, S.B., Wadatkar, A.A., and Kharat, P.B., 2020, Gas sensing behavior of ZnO thick film sensor towards H_2S, NH_3, LPG and CO_2, *J. Phys.: Conf. Ser.*, 1644 (1), 012060.

[81] Jiang, L., Tu, S., Xue, K., Yu, H., and Hou, X., 2021, Preparation and gas-sensing performance of GO/SnO_2/NiO gas-sensitive composite materials, *J. Ceram. Int.*, 47 (6), 7528–7538.

[82] Ge, W., Jiao, S., Chang, Z., He, X., and Li, Y., 2020, Ultrafast response and high selectivity toward acetone vapor using hierarchical structured TiO_2 nanosheets, *ACS Appl. Mater. Interfaces*, 12 (11), 13200–13207.

[83] Tharsika, T., Thanihaichelvan, M., Haseeb, A.S.M.A., and Akbar, S.A., 2019, Highly sensitive and selective ethanol sensor based on ZnO nanorod on SnO_2 thin film fabricated by spray pyrolysis, *Front. Mater.*, 6, 00122.

[84] Liu, P., Wang, J., Jin, H., Ge, M., Zhang, F., Wang, C., Sun, Y., and Dai, N., 2023, SnO_2 mesoporous nanoparticle-based gas sensor for highly sensitive and low concentration formaldehyde detection, *RSC Adv.*, 13 (4), 2256–2264.

[85] Al-Jumaili, B.E., Rzaij, J.M., and Ibraheam, A.S., 2021, Nanoparticles of CuO thin films for room temperature NO_2 gas detection: Annealing time effect, *Mater. Today: Proc.*, 42, 2603–2608.

[86] Shaban, M., Ali, S., and Rabia, M., 2019, Design and application of nanoporous graphene oxide film for CO_2, H_2, and C_2H_2 gases sensing, *J. Mater. Res. Technol.*, 8 (5), 4510–4520.

[87] Goel, N., Kunal, K., Kushwaha, A., and Kumar, M., 2022, Metal oxide semiconductors for gas sensing, *Eng. Rep.*, 5 (6), e12604.

[88] Li, S., Zhang, M., and Wang, H., 2021, Simulation of gas sensing mechanism of porous metal oxide semiconductor sensor based on finite element analysis, *Sci Rep.*, 11 (1), 17158.

[89] Potje-Kamloth, K., 2008, Semiconductor junction gas sensors, *Chem. Rev.*, 108 (2), 367–399.

[90] Jung, G., Shin, W., Hong, S., Jeong, Y., Park, J., Kim, D., Bae, J.H., Park, B.G., and Lee, J.H., 2021, Comparison of the characteristics of semiconductor gas sensors with different transducers fabricated on the same substrate, *Sens. Actuators, B*, 335, 129661.

[91] Isaac, N.A., Pikaar, I., and Biskos, G., 2022, Metal oxide semiconducting nanomaterials for air quality gas sensors: Operating principles, performance, and synthesis techniques, *Microchim. Acta*, 189 (5), 196.

[92] Ijaz, I., Gilani, E., Nazir, A., and Bukhari, A., 2020, Detail review on chemical, physical and green synthesis, classification, characterizations and applications of nanoparticles, *Green Chem. Lett. Rev.*, 13 (3), 223–245.

[93] Badanayak, P., and Vastrad, J.V., 2021, Sol-gel process for synthesis of nanoparticles and applications thereof, *Pharma Innovation*, 10 (8), 1023–1027.

[94] Bokov, D., Turki Jalil, A., Chupradit, S., Suksatan, W., Javed Ansari, M., Shewael, I.H., Valiev, G.H., and Kianfar, E., 2021, Nanomaterial by sol-gel method: Synthesis and application, *Adv. Mater. Sci. Eng.*, 2021 (1), 5102014.

[95] Latif, W.A., and AL-Owaidi, M.N., 2023, Review article: Sol-gel method, "Synthesis and applications", *WJAETS*, 8 (2), 160–166.

[96] Parashar, M., Shukla, V.K., and Singh, R., 2020, Metal oxides nanoparticles via sol–gel method: A review on synthesis, characterization and applications, *J. Mater. Sci.: Mater. Electron.*, 31 (5), 3729–3749.

[97] Shaposhnik, A.V., Shaposhnik, D.A., Turishchev, S.Y., Chuvenkova, O.A., Ryabtsev, S.V., Vasiliev,

A.A., Vilanova, X., Hernandez-Ramirez, F., and Morante, J.R., 2019, Gas sensing properties of individual SnO_2 nanowires and SnO_2 sol-gel nanocomposites, *Beilstein J. Nanotechnol.*, 10, 1380–1390.

[98] Patel, M., Mishra, S., Verma, R., and Shikha, D., 2022, Synthesis of ZnO and CuO nanoparticles via sol gel method and its characterization by using various technique, *Discover Mater.*, 2 (1), 1.

[99] Han, T.H., Bak, S.Y., Kim, S., Lee, S.H., Han, Y.J., and Yi, M., 2021, Decoration of CuO NWs gas sensor with ZnO NPs for improving NO_2 sensing characteristics, *Sensors*, 21 (6), 2103.

[100] Rendón-Angeles, J.C., and Seong, G., 2023, Editorial for the special issue: Hydrothermal synthesis of nanoparticles, *Nanomaterials*, 13 (9), 1463.

[101] Jalouli, B., Abbasi, A., and Musavi Khoei, S.M., 2019, A comment on: "Conventional and microwave hydrothermal synthesis and application of functional materials: A review", *Materials*, 12 (21), 3631.

[102] Hassan, E., Al-saidi, M.H., Rana, J.A., and Thahab, S.M., 2022, Preparation and characterization of ZnO nano-sheets prepared by different depositing methods, *Iraqi J. Sci.*, 63 (2), 538–547.

[103] San, X., Zhang, Y., Zhang, L., Wang, G., Meng, D., Cui, J., and Jin, Q., 2022, One-step hydrothermal synthesis of 3D interconnected rGO/In_2O_3 heterojunction structures for enhanced acetone detection, *Chemosensors*, 10 (7), 270.

[104] Sakthivel, B., and Nammalvar, G., 2019, Selective ammonia sensor based on copper oxide/reduced graphene oxide nanocomposite, *J. Alloys Compd.*, 788, 422–428.

[105] Claros, M., Gràcia, I., Figueras, E., and Vallejos, S., 2022, Hydrothermal synthesis and annealing effect on the properties of gas-sensitive copper oxide nanowires, *Chemosensors*, 10 (9), 353.

[106] Zhang, K., Suh, J.M., Lee, T.H., Cha, J.H., Choi, J.W., Jang, H.W., Varma, R.S., and Shokouhimehr, M., 2019, Copper oxide–graphene oxide nanocomposite: Efficient catalyst for hydrogenation of nitroaromatics in water, *Nano Convergence*, 6 (1), 6.

[107] Huang, M., Wang, Y., Ying, S., Wu, Z., Liu, W., Chen, D., and Peng, C., 2021, Synthesis of Cu_2O-modified reduced graphene oxide for NO_2 sensors, *Sensors*, 21 (6), 1958.

[108] Bai, H., Guo, H., Wang, J., Dong, Y., Liu, B., Xie, Z., Guo, F., Chen, D., Zhang, R., and Zheng, Y., 2021, A room-temperature NO_2 gas sensor based on CuO nanoflakes modified with rGO nanosheets, *Sens. Actuators, B*, 337, 129783.

[109] Al-Harbi, N., and Abd-Elrahman, N.K., 2024, Physical methods for preparation of nanomaterials, their characterization and applications: A review, *J. Umm Al-Qura Univ. Appl. Sci.*, 2024, s43994-024-00165-7.

[110] Fazio, E., Gökce, B., De Giacomo, A., Meneghetti, M., Compagnini, G., Tommasini, M., Waag, F., Lucotti, A., Zanchi, C.G., Ossi, P.M., Dell'Aglio, M., D'Urso, L., Condorelli, M., Scardaci, V., Biscaglia, F., Litti, L., Gobbo, M., Gallo, G., Santoro, M., Trusso, S., and Neri, F., 2020, Nanoparticles engineering by pulsed laser ablation in liquids: Concepts and applications, *Nanomaterials*, 10 (11), 2317.

[111] Piotto, V., Litti, L., and Meneghetti, M., 2020, Synthesis and shape manipulation of anisotropic gold nanoparticles by laser ablation in solution, *J. Phys. Chem. C*, 124 (8), 4820–4826.

[112] Bin, K., Kumar, P., Malik, M.A., and Singh, J., 2021, A comprehensive tutorial on the pulsed laser deposition technique and developments in the fabrication of low dimensional systems and nanostructures, *J. Emergent Mater.*, 4 (3), 737–754.

[113] Haider, A.J., Alawsi, T., Haider, M.J., Taha, B.A., and Marhoon, H.A., 2022, A comprehensive review on pulsed laser deposition technique to effective nanostructure production: Trends and challenges, *Opt. Quantum Electron.*, 54 (8), 488.

[114] Fadhil, F.A., Sultan, F.I., Haider, A.J., and Rsool, R.A., 2019, Preparation of poison gas sensor from WO_3 nanostructure by pulsed laser deposition, *J. AIP Conf. Proc.*, 2190 (1), 020056.

[115] Khudiar, A.I., and Ofui, A.M., 2021, Effect of pulsed laser deposition on the physical properties

of ZnO nanocrystalline gas sensors, *Opt. Mater.*, 115, 111010.

[116] Mhadhbi, M., 2021, Modelling of the high-energy ball milling process, *Adv. Mater. Phys. Chem.*, 11 (1), 31–44.

[117] Piras, C.C., Fernández-Prieto, S., and De Borggraeve, W.M., 2019, Ball milling: A green technology for the preparation and functionalisation of nanocellulose derivatives, *J. Nanoscale Adv.*, 1 (3), 937–947.

[118] El-Eskandarany, M.M., Al-Hazza, A., Al-Hajji, L.A., Ali, N., Al-Duweesh, A.A., Banyan, M., and Al-Ajmi, F., 2021, Mechanical milling: A superior nanotechnological tool for fabrication of nanocrystalline and nanocomposite materials, *Nanomaterials*, 11 (10), 2484.

[119] Jamkhande, P.G., Ghule, N.W., Bamer, A.H., and Kalaskar, M.G., 2019, Metal nanoparticles synthesis: An overview on methods of preparation, advantages and disadvantages, and applications, *J. Drug Delivery Sci. Technol.*, 53, 101174.

[120] Khatibani, A.B., 2021, Investigation of gas sensing property of zinc oxide thin films deposited by sol-gel method: Effects of molarity and annealing temperature, *Indian J. Phys.*, 95 (2), 243–252.

[121] Zhang, D., Pan, W., Tang, M., Wang, D., Yu, S., Mi, Q., Pan, Q., and Hu, Y., 2023, Diversiform gas sensors based on two-dimensional nanomaterials, *Nano Res.*, 16 (10), 11959–11991.

[122] Sapkota, R., Duan, P., Kumar, T., Venkataraman, A., and Papadopoulos, C., 2021, Thin film gas sensors based on planetary ball-milled zinc oxide nanoinks: Effect of milling parameters on sensing performance, *Appl. Sci.*, 11 (20), 9676.

[123] Vajhadin, F., Mazloum-Ardakani, M., and Amini, A., 2021, Metal oxide-based gas sensors for the detection of exhaled breath markers, *Med. Devices Sens.*, 4 (1), e10161.

[124] Elwood, M., 2021, The scientific basis for occupational exposure limits for hydrogen sulphide—A critical commentary, *Int. J. Environ. Res. Public Health*, 18 (6), 2866.

[125] Duc, C., Boukhenane, M.L., Wojkiewicz, J.L., and Redon, N., 2020, Hydrogen sulfide detection by sensors based on conductive polymers: A review, *Front. Mater.*, 7, 00215.

[126] Park, K.R., Cho, H.B., Lee, J., Song, Y., Kim, W.B., and Choa, Y.H., 2020, Design of highly porous SnO_2-CuO nanotubes for enhancing H_2S gas sensor performance, *Sens. Actuators, B*, 302, 127179.

[127] Kim, J.H., Mirzaei, A., Zheng, Y., Lee, J.H., Kim, J.Y., Kim, H.W., and Kim, S.S., 2019, Enhancement of H_2S sensing performance of p-CuO nanofibers by loading p-reduced graphene oxide nanosheets, *Sens. Actuators, B*, 281, 453–461.

[128] Shujah, T., Ikram, M., Butt, A.R., Shahzad, M.K., Rashid, K., Zafar, Q., and Ali, S., 2020, H_2S Gas sensor based on WO_3 nanostructures synthesized via aerosol assisted chemical vapor deposition technique, *Nanosci. Nanotechnol. Lett.*, 11 (9), 1247–1256.

[129] Zhang, W., Yang, F., Xu, J., Gu, C., and Zhou, K., 2020, Sensitive carbon monoxide gas sensor based on chemiluminescence on Nano-Au/Nd_2O_3-$Ca_3Nd_2O_6$: Working condition optimization by response surface methodology, *ACS Omega*, 5 (32), 20034–20041.

[130] Kinoshita, H., Türkan, H., Vucinic, S., Naqvi, S., Bedair, R., Rezaee, R., and Tsatsakis, A., 2020, Carbon monoxide poisoning, *Toxicol. Rep.*, 7, 169–173.

[131] Sinha, S., Barman, P.B., and Hazra, S.K., 2023, Probing the electronic properties of chemically synthesised doped and undoped graphene derivative, *Mater. Sci. Eng., B*, 287, 116145.

[132] Hjiri, M., Bahanan, F., Aida, M.S., El Mir, L., and Neri, G., 2020, High performance CO gas sensor based on ZnO nanoparticles, *J. Inorg. Organomet. Polym. Mater.*, 30 (10), 4063–4071.

[133] Basu, A.K., Chauhan, P.S., Awasthi, M., and Bhattacharya, S., 2019, α-Fe_2O_3 loaded rGO nanosheets based fast response/recovery CO gas sensor at room temperature, *Appl. Surf. Sci.*, 465, 56–66.

[134] Molavi, R., and Sheikhi, M.H., 2019, Facile wet chemical synthesis of Al doped CuO nanoleaves for carbon monoxide gas sensor applications, *J. Mater. Sci. Semicond. Process.*, 106, 104767.

[135] Dhage, S.B., Patil, V.L., Patil, P.S., Ryu, J., Patil, D.R., and Malghe, Y.S., 2021, Synthesis and characterization of CuO-SnO_2 nanocomposite for CO gas sensing application, *Mater. Lett.*, 305, 130831.

[136] Abinaya, M., Pal, R., and Sridharan, M., 2019, Highly sensitive room temperature hydrogen sensor based on undoped SnO_2 thin films, *Solid State Sci.*, 95, 105928.

[137] Chauhan, P.S., and Bhattacharya, S., 2019, Hydrogen gas sensing methods, materials, and approach to achieve parts per billion level detection: A review, *Int. J. Hydrogen Energy*, 44 (47), 26076–26099.

[138] Lu, S., Zhang, Y., Liu, J., Li, H.Y., Hu, Z., Luo, X., Gao, N., Zhang, B., Jiang, J., Zhong, A., Luo, J., and Liu, H., 2021, Sensitive H_2 gas sensors based on SnO_2 nanowires, *Sens. Actuators, B*, 345, 130334.

[139] Das, S., Roy, S., and Sarkar, C.K., 2021, Performance improvement of n-ZnO/p-rGO heterojunction based room temperature hydrogen gas sensor, *J. IEEE Sens. Lett.*, 5 (5), 1–4.

[140] Chang, C.H., Chou, T.C., Chen, W.C., Niu, J.S., Lin, K.W., Cheng, S.Y., Tsai, J.H., and Liu, W.C., 2020, Study of a WO_3 thin film based hydrogen gas sensor decorated with platinum nanoparticles, *Sens. Actuators, B*, 317, 128145.

[141] Zeng, H., Zhang, G., Nagashima, K., Takahashi, T., Hosomi, T., and Yanagida, T., 2021, Metal–oxide nanowire molecular sensors and their promises, *Chemosensors*, 9 (2), 41.

[142] Bai, H., Guo, H., Feng, C., Wang, J., Liu, B., Xie, Z., Guo, F., Chen, D., Zhang, R., and Zheng, Y., 2022, Highly responsive and selective ppb-level NO_2 gas sensor based on porous Pd-functionalized CuO/rGO at room temperature, *J. Mater. Chem. C*, 10 (10), 3756–3769.

[143] Agrawal, A.V., Kumar, N., and Kumar, M., 2021, Strategy and future prospects to develop room-temperature-recoverable NO_2 gas sensor based on two-dimensional molybdenum disulfide, *Nano-Micro Lett.*, 13 (1), 38.

[144] Kumar, S., Pavelyev, V., Mishra, P., Tripathi, N., Sharma, P., and Calle, F., 2020, A review on 2D transition metal di-chalcogenides and metal oxide nanostructures based NO_2 gas sensors, *Mater. Sci. Semicond. Process.*, 107, 104865.

[145] Tyagi, S., Chaudhary, M., Ambedkar, A.K., Sharma, K., Gautam, Y.K., and Singh, B.P., 2022, Metal oxide nanomaterial-based sensors for monitoring environmental NO_2 and its impact on the plant ecosystem: A review, *Sens. Diagn.*, 1 (1), 106–129.

[146] Sivakumar, R., Krishnamoorthi, K., Vadivel, S., and Govindasamy, S., 2021, Progress towards a novel NO_2 gas sensor based on SnO_2/RGO hybrid sensors by a facial hydrothermal approach, *Diamond Relat. Mater.*, 116, 108418.

[147] Wang, Y., Liu, L., Sun, F., Li, T., Zhang, T., and Qin, S., 2021, Humidity-insensitive NO_2 sensors based on SnO_2/rGO composites, *Front. Chem.*, 9, 681313.

[148] Petrov, V.V., Ivanishcheva, A.P., Volkova, M.G., Storozhenko, V.Y., Gulyaeva, I.A., Pankov, I.V., Volochaev, V.A., Khubezhov, S.A., and Bayan, E.M., 2022, High gas sensitivity to nitrogen dioxide of nanocomposite ZnO-SnO_2 films activated by a surface electric field, *Nanomaterials*, 12 (12), 2025.

[149] Kazanskiy, N.L., Butt, M.A., and Khonina, S.N., 2021, Carbon dioxide gas sensor based on polyhexamethylene biguanide polymer deposited on silicon nano-cylinders metasurface, *Sensors*, 21 (2), 378.

[150] Rezk, M.Y., Sharma, J., and Gartia, M.R., 2020, Nanomaterial-based CO_2 sensors, *Nanomaterials*, 10 (11), 2251.

[151] Gerbreders, V., Krasovska, M., Mihailova, I., Kostjukevics, J., Sledevskis, E., Ogurcovs, A., Gerbreders, A., and Bulanovs, A., 2021, Metal oxide nanostructure-based gas sensor for carbon dioxide detection, *Latv. J. Phys. Tech. Sci.*, 58 (5), 15–26.

[152] Lee, M.A., Zaki, S.E., Ertugrul, S., Yilmaz, M., and Eker, Y.R., 2020, Fast response of CO_2 room temperature gas sensor based on mixed-valence phases in Molybdenum and Tungsten Oxide nanostructured thin films, *Ceram. Int.*, 46 (7), 9839–9853.

[153] Lee, Z.Y., bin Hawari, H.F., bin Djaswadi, G.W., and Kamarudin, K., 2021, A highly sensitive room temperature CO_2 gas sensor based on SnO_2-rGO hybrid composite, *Materials*, 14 (3), 522.

[154] Kohale, A., 2024, Study of CO_2 sensing properties of SnO_2-CuO thick films, *Int. J. Res. Anal. Rev.*, 11 (1), 74–78.

[155] Kanaparthi, S., and Singh, S.G., 2019, Chemiresistive sensor based on zinc oxide nanoflakes for CO_2 detection, *ACS Appl. Nano Mater.*, 2 (2), 700–706.

[156] Yu, W., Shen, Z., Peng, F., Lu, Y., Ge, M., Fu, X., Sun, Y., Chen, X., and Dai, N., 2019, Improving gas sensing performance by oxygen vacancies in sub-stoichiometric WO_{3-x}, *RSC Adv.*, 9 (14), 7723–7728.

[157] Radhakrishnan, J.K., Kumara, M., and Geetika, G., 2021, Effect of temperature modulation, on the gas sensing characteristics of ZnO nanostructures, for gases O_2, CO and CO_2, *Sens. Int.*, 2, 100059.

[158] Al-Hashem, M., Akbar, S., and Morris, P., 2019, Role of oxygen vacancies in nanostructured metal-oxide gas sensors: A review, *Sens. Actuators, B*, 301, 126845.

[159] Raju, P., and Li, Q., 2022, Review—Semiconductor materials and devices for gas sensors, *J. Electrochem. Soc.*, 169 (5), 057518.

[160] Bag, A., and Lee, N.E., 2019, Gas sensing with heterostructures based on two-dimensional nanostructured materials: A review, *J. Mater. Chem. C*, 7 (43), 13367–13383.

[161] Liu, Y., Xiao, S., and Du, K., 2021, Chemiresistive gas sensors based on hollow heterojunction: A review, *Adv. Mater. Interfaces*, 8 (12), 2002122.

[162] Barreca, D., Maccato, C., and Gasparotto, A., 2022, Metal oxide nanosystems as chemoresistive gas sensors for chemical warfare agents: A focused review, *Adv. Mater. Interfaces*, 9 (14), 2102525.

[163] Li, Z., Li, H., Wu, Z., Wang, M., Luo, J., Torun, H., Hu, P.A., Yang, C., Grundmann, M., Liu, X., and Fu, Y.Q., 2019, Advances in designs and mechanisms of semiconducting metal oxide nanostructures for high-precision gas sensors operated at room temperature, *Mater. Horiz.*, 6 (3), 470–506.

[164] Subha, P.P., and Jayaraj, M.K., 2019, Enhanced room temperature gas sensing properties of low temperature solution processed ZnO/CuO heterojunction, *BMC Chem.*, 13 (1), 4.

[165] Mathew, M., Shinde, P.V., Samal, R., and Rout, C.S., 2021, A review on mechanisms and recent developments in p-n heterojunctions of 2D materials for gas sensing applications, *J. Mater. Sci.*, 56 (16), 9575–9604.

[166] Zhang, J., Ma, S., Wang, B., and Pei, S., 2021, Hydrothermal synthesis of SnO_2-CuO composite nanoparticles as a fast-response ethanol gas sensor, *J. Alloys Compd.*, 8861, 61299.

[167] Yang, S., Lei, G., Xu, H., Lan, Z., Wang, Z., and Gu, H., 2021, Metal oxide based heterojunctions for gas sensors: A review, *Nanomaterials*, 11 (4), 1026.

[168] Gai, L.Y., Lai, R.P., Dong, X.H., Wu, X., Luan, Q.T., Wang, J., Lin, H.F., Ding, W.H., and Wu, G.L., and Xie, W.F., 2022, Recent advances in ethanol gas sensors based on metal oxide semiconductor heterojunctions, *Rare Met.*, 41 (6), 1818–1842.

[169] Du, K., Zhang, L., Shan, H., Dong, S., Shen, X., and Li, G., 2024, Synthesis of ZnO nanorods loaded with SnO_2 cubes and the mechanism of improved ethanol sensing performance with DFT calculation, *Mater. Sci. Semicond. Process.*, 178, 108429.

[170] Xue, D., Wang, J., Wang, Y., Sun, G., Cao, J., Bala, H., and Zhang, Z., 2019, Enhanced methane sensing properties of WO_3 nanosheets with dominant exposed (200) facet via loading of SnO_2 nanoparticles, *Nanomaterials*, 9 (3), 351.

[171] Yang, B., Myung, N.V., and Tran, T.T., 2021, 1D metal oxide semiconductor materials for chemiresistive gas sensors: A review, *Adv. Electron. Mater.*, 7 (9), 2100271.

[172] Hashemi Karouei, S.F., and Milani Moghaddam, H., 2019, p-p Heterojunction of polymer/hierarchical mesoporous $LaFeO_3$ microsphere as CO_2 gas sensing under high humidity, *Appl. Surf. Sci.*, 479, 1029–1038.

[173] Sarode, H.A., Barai, D.P., Bhanvase, B.A., Ugwekar, R.P., and Saharan, V., 2020, Investigation on preparation of graphene oxide-CuO nanocomposite based nanofluids with the aid of ultrasound assisted method for intensified heat transfer properties, *Mater. Chem. Phys.*, 251, 123102.

[174] Gou, X., Wang, G., Yang, J., Park, J., and Wexler, D., 2008, Chemical synthesis, characterisation and gas sensing performance of copper oxide nanoribbons, *J. Mater. Chem.*, 18 (9), 965–969.

[175] Yin, L., Wang, H., Li, L., Li, H., Chen, D., and Zhang, R., 2019, Microwave-assisted preparation of hierarchical CuO@rGO nanostructures and their enhanced low-temperature H_2S-sensing performance, *Appl. Surf. Sci.*, 476, 107–114.

[176] Liu, Y., Ma, H., Han, X.X., and Zhao, B., 2021, Metal-semiconductor heterostructures for surface-enhanced Raman scattering: Synergistic contribution of plasmons and charge transfer, *Mater. Horiz.*, 8 (2), 370–382.

[177] Yu, X., and Sivula, K., 2017, Layered 2D semiconducting transition metal dichalcogenides for solar energy conversion, *Curr. Opin. Electrochem.*, 2 (1), 97–103.

[178] Kushwaha, A., Kumar, R., and Goel, N., 2024, Chemiresistive gas sensors beyond metal oxides: Using ultrathin two-dimensional nanomaterials, *FlatChem*, 43, 100584.

[179] Shao, G., Xu, Y., and Liu, S., 2019, Controllable preparation of 2D metal-semiconductor layered metal dichalcogenides heterostructures, *Sci. China: Chem.*, 62 (3), 295–298.

[180] Kumar, R., Liu, X., Zhang, J., and Kumar, M., 2020, Room-temperature gas sensors under photoactivation: from metal oxides to 2D materials, *Nano-Micro Lett.*, 12 (1), 164.

[181] Sabry, R.S., Agool, I.R., and Abbas, A.M., 2019, Hydrothermal synthesis of In_2O_3:Ag nanostructures for NO_2 gas sensor, *Silicon*, 11 (5), 2475–2478.

[182] Karthik, T.V.K., Olvera, M.D.L., Maldonado, A., and Gómez Pozos, H., 2016, CO gas sensing properties of pure and Cu-incorporated SnO_2 nanoparticles: A study of cu-induced modifications, *Sensors*, 16 (8), 1283.